



저작자표시-비영리-변경금지 2.0 대한민국

이용자는 아래의 조건을 따르는 경우에 한하여 자유롭게

- 이 저작물을 복제, 배포, 전송, 전시, 공연 및 방송할 수 있습니다.

다음과 같은 조건을 따라야 합니다:



저작자표시. 귀하는 원저작자를 표시하여야 합니다.



비영리. 귀하는 이 저작물을 영리 목적으로 이용할 수 없습니다.



변경금지. 귀하는 이 저작물을 개작, 변형 또는 가공할 수 없습니다.

- 귀하는, 이 저작물의 재이용이나 배포의 경우, 이 저작물에 적용된 이용허락조건을 명확하게 나타내어야 합니다.
- 저작권자로부터 별도의 허가를 받으면 이러한 조건들은 적용되지 않습니다.

저작권법에 따른 이용자의 권리는 위의 내용에 의하여 영향을 받지 않습니다.

이것은 [이용허락규약\(Legal Code\)](#)을 이해하기 쉽게 요약한 것입니다.

[Disclaimer](#)

이학박사 학위논문

**Macrophage-derived endotrophin
supports tumor migration potentials in
thyroid cancer**

종양관련 대식세포에서 유래되는 endotrophin
이 갑상선암 미세환경에 미치는 역할에 대한 연구

2023년 8월

서울대학교 대학원

의학과 중개의학 전공

신효식

중앙관련 대식세포에서 유래되는
endotrophin이 갑상선암 미세환경에
미치는 역할에 대한 연구

지도 교수 박도준

이 논문을 이학박사 학위논문으로 제출함
2023년 4월

서울대학교 대학원
의학과 중개의학 전공
신효식

신효식의 이학박사 학위论문을 인준함
2023년 7월

위원장 이미옥 (인)

부위원장 박도준 (인)

위원 배윤수 (인)

위원 조선욱 (인)

위원 김재범 (인)

ABSTRACT

Macrophage-derived endotrophin supports tumor migration potentials in thyroid cancer

Hyo Shik Shin

Department of Translational Medicine

The Graduate School

Seoul National University

(Directed by Prof. Do Joon Park, M.D, Ph.D.)

Endotrophin (ETP), a cleaved fragment of the C5 domain of the Type VI collagen $\alpha 3$ (COL6A3), has been shown to play pro-tumorigenic roles in breast and liver cancers. However, the actions of ETP in the tumor microenvironment (TME) remain undetermined. I aimed to investigate the role and mechanism of ETP in the TME of macrophage-enriched thyroid cancer. Mouse thyroid tumors were co-stained with anti-ETP and anti-CD163 antibodies to clarify the origin of ETP in the TME of thyroid cancer. Immunofluorescence staining showed that ETP and anti-CD163 positive macrophages co-localized in the peritumoral area. The protumorigenic functions of ETP have also been studied. Conditioned medium from co-cultures of FRO or BCPAP (human thyroid cancer cell lines) with THP-1

cells (human monocytic cell line) was harvested and then FRO or BCPAP cells were treated with it. Treatment with conditioned medium from co-cultures increased cell migration potentials compared to that of single cells alone, and the anti-ETP neutralizing antibody reduced these effects. Moreover, MMP-9 or MMP-14, the candidates of COL6A3 protease that produces ETP, increased in THP-1 cells by treatment with conditioned medium. Additionally, treatment with conditioned medium from MMP-9 or MMP-14 inhibitor-treated co-cultures of FRO or BCPAP cells and THP-1 cells decreased the cancer cell migration potential compared to the control conditioned medium, and these effects were reversed by treatment with ETP. The RNA-sequencing dataset of ETP-treated FRO cells showed that genes related to cell migration were the most differentially expressed. In an in vivo study, deficiency of *Col6a3* resulted in reduced tumor growth. Further, in analyzing immune response in tumors, the mRNA expression of *Cd4*, *Cd8*, and *Cd80* was increased in COL6A3-KO mice tumors. Taken together, macrophage-derived ETP supports the pro-metastatic potential of human thyroid cancer cells and the immune inhibitory response in the TME.

Keywords: Endotrophin; tumor microenvironment; thyroid cancer; collagen 6 alpha 3; macrophage

Student Number: 2018-35950

CONTENTS

ABSTRACT	i
CONTENTS	iii
LIST OF FIGURES	vi
LIST OF TABLES	viii
1. INTRODUCTION	1
1.1. Tumor Microenvironment	1
1.2. Tumor-Associated Macrophages in the Tumor Microenvironment (TME)	3
1.3. Targeting Tumor-Associated Macrophages (TAMs) in the Tumor Microenvironment (TME)	6
1.4. The Thyroid Tumor Microenvironment	8
1.5. Suggested oncogenic role of Collagen Type VI Alpha 3 in TME.....	9
1.6. ECM Interactions in the Tumor Microenvironment of Advanced Thyroid Cancer.....	10
1.7. Aim of the study	12
2. MATERIALS AND METHODS	13
2.1. Animal experiments	13
2.2. Cell culture	13
2.3. Harvest of ETP conditioned medium	14
2.4. Harvest of anti-ETP antibody medium	14

2.5. Preparation of conditioned medium	15
2.6. Immunohistochemistry staining	16
2.7. Immunofluorescent staining	16
2.8. Real-time PCR analysis	17
2.9. Western blotting analysis	17
2.10. Cell migration assay	18
2.11. Cell viability assay	18
2.12. Isolation of bone marrow-derived monocytes/ macrophages	19
2.13. RNA sequencing	20
2.14. Statistical analysis	20
3. RESULTS	23
3.1. Expression and Association of Endotrophin and CD163-positive TAM in Human Thyroid Cancer Tissues	23
3.2. Peritumoral Co-localization of Endotrophin Expressions with CD163-Positive Macrophage Concentration: Evidence from a Syngeneic Mouse Model of ATC	30
3.3. Enhanced ETP Production from Macrophages via Thyroid Cancer Cells-Macrophage Interactions	33
3.4. The effects of ETP on Cell Viability in Thyroid Cancer Cells	36
3.5. The Effects of ETP on Thyroid Cancer Cell Migration	38
3.6. Molecular Mechanism of ETP-Mediated Cancer Cell Migration: Insight from transcriptomic analysis	44
3.7. Comparing Tumor Growth and Microenvironments in an	

Orthotopic Syngeneic Animal Model using COL6A3-Deficient Mice	49
3.8. ETP Interactions with the Tumor Microenvironment in Human Thyroid Cancer	58
3.9. MMP-9 and MMP-14 dependent production of ETP in macrophages	66
4. DISCUSSION	72
5. REFERENCES	80
국문초록	96
감사의 글	99

LIST OF FIGURE

Figure 1. Expression of ETP in various types of human thyroid tissue.

Figure 2. Regions of ETP-expressed in thyroid cancer tissues.

Figure 3. Expression of ETP in macrophage-enriched thyroid TME.

Figure 4. Co-localization of ETP expression and M2 macrophages in the TME of thyroid cancer.

Figure 5. Upregulation of COL6A3 gene in THP-1 cells by thyroid cancer cell CM.

Figure 6. Macrophage-derived ETP in vitro.

Figure 7. ETP effects on thyroid cancer cell proliferation.

Figure 8. ETP supports the migration potentials of thyroid cancer cells.

Figure 9. Macrophage derived ETP supports the migration potentials of thyroid cancer cells.

Figure 10. Col6a3-KO mice bone marrow monocytes CoCM reduces the migration potentials of thyroid cancer cells.

Figure 11. ETP has no effect of normal thyroid cell migration potential.

Figure 12. Molecular characteristics in epithelial mesenchymal transition related genes by RNA-sequencing.

Figure 13. Expression of cell migration related genes in CoCM-treated FRO cells.

Figure 14. Analysis of oncogenic signaling pathways.

Figure 15. Reduced thyroid tumor growth in COL6A3-KO mice.

Figure 16. Expression of various cell types in mouse thyroid cancer.

Figure 17. Correlation of tumor volume and immune cells.

Figure 18. Expression of immune cell markers in mouse thyroid cancer.

Figure 19. Expression of COL6A3 in human thyroid cancer.

Figure 20. GO analysis of RNA-sequencing data in PTC.

Figure 21. Correlation between COL6A3 and immune related genes in PTC.

Figure 22. GO analysis of RNA-sequencing data in ATC.

Figure 23. Correlation between COL6A3 and immune related genes in ATC.

Figure 24. Analysis of MMPs associated with COL6A3 in thyroid cancers.

Figure 25. Expression of MMPs in CM-stimulated THP-1 cells.

Figure 26. MMP-9 and MMP-14 cleaved COL6A3 to produce ETP in thyroid cancer cells CM-stimulated THP-1 cells.

LIST OF TABLES

Table 1. Primer sequences

Table 2. Immunohistochemical staining of ETP in various human thyroid tissues

Table 3. Clinical characteristics of patients with thyroid cancer patients based on ETP expression

1. Introduction

1.1. Tumor Microenvironment

The tumor microenvironment (TME) consists of a heterogeneous complex comprising tumor cells, fibroblasts, endothelial cells, extracellular matrix components (ECM), and immune cells like T-cells and macrophages (1-3). Immune cells within the TME play a crucial role in tumor growth, invasion, and metastasis (4). The impact of immune cells on cancer progression can be either promoting or inhibitory, depending on their cell type and function (5-8).

The immune system recognizes and responds to foreign antigens, such as those found on pathogens or cancer cells, while maintaining tolerance to self-antigens present on the body's own cells (9). T lymphocytes, or T-cells, play a pivotal role in the immune response by recognizing antigens and activating other immune cells to mount a defense. T-cell activation begins with the binding of T-cell receptors (TCRs) to antigens presented by antigen-presenting cells (APCs) (10). This binding event initiates signaling pathways that lead to T-cell activation, proliferation, and differentiation into effector cells capable of eliminating the target antigen. In cancer, the immune system may fail to recognize and eliminate cancer cells due to factors such as the presence of immune-suppressive molecules or mutations affecting antigen expression (11, 12). Immunotherapy aims to enhance T-cell activation and function, thus boosting the immune response against cancer by targeting these

mechanisms (13).

Cancer immunotherapy has been extensively studied and utilized for many years. It can be broadly classified into two types: active and passive immunotherapies (14). Active immunotherapy stimulates the immune system to recognize and attack cancer cells (15). Examples include therapeutic cancer vaccines (16), designed to activate the body's immune system against cancer. Passive immunotherapy involves using pre-made immune system components, such as monoclonal antibodies, to directly target cancer cells (17). CAR-T cell therapy genetically modifies a patient's T-cells to identify and eliminate cancer cells, while targeted antibody therapies utilize monoclonal antibodies to bind to specific molecules on cancer cell surfaces, inhibiting their growth (18). The advent of immune checkpoint inhibitors significantly improved the efficacy of immunotherapy for solid cancers. Immune checkpoint inhibitors work by blocking signals used by cancer cells to evade the immune system, enabling more effective recognition and attack by immune cells (19-21). Examples of immune checkpoint inhibitors include CTLA-4 inhibitors (ipilimumab) and PD-1 inhibitors (pembrolizumab and nivolumab) (22)(23). CTLA-4 is a protein on T-cells that regulates the immune response by binding to CD80/CD86 proteins on APCs (24, 25). Blocking CTLA-4 allows T-cells to remain activated and more effectively attack cancer cells (26, 27). PD-1 is another protein on T-cells that interacts with PD-L1 and PD-L2 proteins on tumor cells (28, 29). This interaction inhibits T-cell function, enabling tumors to evade the immune system.

Blocking PD-1 with drugs like pembrolizumab and nivolumab maintains T-cell activation. Immunotherapy can be less toxic than chemotherapy or targeted therapies as it activates the body's immune system to fight cancer cells instead of directly attacking them, leading to fewer side effects by specifically targeting cancer cells while sparing healthy cells (30, 31).

The tumor microenvironment (TME) can be classified into "hot" or "cold" based on T cell infiltration. Hot tumors exhibit high levels of T cell infiltration, indicating an active immune response against the tumor. In contrast, cold tumors show little to no T cell infiltration, suggesting a lack of immune response (32, 33). As a result, hot tumors generally display greater responsiveness to immunotherapy, such as anti-PD-1/PD-L1 therapeutics, which activate T cells to target the tumor. Conversely, patients with cold tumors typically exhibit resistance to immunotherapy. Moreover, blocking immune checkpoints can induce immune-related adverse effects, resulting from the hyperactivation of the immune system and subsequent autoimmune reactions (34, 35).

1.2. Tumor-Associated Macrophages in the Tumor Microenvironment (TME)

Macrophages are crucial immune cells that contribute to tumor growth, metastasis, and angiogenesis in the TME (5, 36). Under normal conditions, macrophages originate from the bone marrow and migrate to tumor sites, where they differentiate into M1 and M2 macrophages (37). M1 macrophages

exhibit anti-tumor effects by releasing pro-inflammatory cytokines and chemokines, including interleukin (IL)-12, IL-23, tumor necrosis factor-alpha (TNF- α), and inducible nitric oxide synthase (iNOS). Activation of M1 macrophages occurs through interferon gamma (IFN- γ) and lipopolysaccharides (LPS), which recruit and activate other immune cells, enhancing their cytotoxic activity against cancer cells within the TME (36, 38). IFN- γ is a cytokine that plays a critical role in the immune response to infections by activating macrophages, stimulating the production of reactive oxygen species (ROS) and cytokines such as IL-1 β (39). Conversely, IL-4 is an anti-inflammatory cytokine that inhibits ROS and IL-1 β production by macrophages (40). IL-4 also induces the differentiation of macrophages into M2 macrophages, characterized by their involvement in tissue repair and remodeling. M2 macrophages express high levels of mannose receptor 1 (MR-1), facilitating pathogen phagocytosis (41, 42). Additionally, M2 macrophages can be induced by macrophage colony-stimulating factor (M-CSF) (42), IL-10 (43), and transforming growth factor beta (TGF- β) (44). These stimuli lead to increased expression of pro-inflammatory chemokines, such as CCL2 (45), CCL17 (46), CCL18 (47), and CCL22 (48), promoting monocyte differentiation into M2 macrophages and enhancing their anti-inflammatory and pro-tumorigenic functions (5, 49). M2 macrophages express specific markers associated with their immunosuppressive and tissue repair functions, including arginase 1 (ARG1), CD163, and CD206 (50, 51). Consequently, M2 macrophages in the TME facilitate tumor growth,

angiogenesis, and immune response suppression against cancer cells.

In the TME, M2 macrophages are commonly referred to as tumor-associated macrophages (TAMs), and high densities of TAMs in cancer tissues have been associated with advanced stages of breast, lung, liver, bladder, and thyroid cancers (52-56). Extensive studies have reported that TAMs contribute to tumor growth, angiogenesis, inflammation, and extracellular matrix (ECM) remodeling through the secretion of various cytokines (103). TAM-secreted TGF- β , via SMAD signaling, has demonstrated effects on tumor growth and progression (104). IL-6, secreted by TAMs, can activate STAT3 signaling in cancer cells, promoting tumorigenesis and tumor progression (105). Additionally, TNF- α can stimulate the growth and survival of cancer cells by activating NF- κ B signaling pathways, crucial for cancer cell proliferation and survival (106). TAMs have been found to produce vascular endothelial growth factor (VEGF), a cytokine that plays a pivotal role in promoting angiogenesis and directly influencing the survival and growth of cancer cells (100). Platelet-derived growth factor (PDGF), a protein promoting blood vessel growth, is also produced by TAMs, supporting tumor growth and dissemination (107). Tumor-associated macrophages (TAMs) contribute to extracellular matrix (ECM) remodeling by secreting enzymes known as matrix metalloproteinases (MMPs), which degrade ECM proteins like collagen and fibronectin. The activity of MMPs promotes cell migration and invasion, facilitating the movement of cells through the tissue (37). Consequently, it is crucial to

comprehend the role of TAMs and the cytokines derived from TAMs in the tumor microenvironment (TME) to develop effective strategies for cancer immunotherapy.

1.3. Targeting Tumor-Associated Macrophages (TAMs) in the Tumor Microenvironment (TME)

TAMs play a crucial role in the TME by promoting immunosuppression through various mechanisms. These mechanisms involve the production of immunosuppressive cytokines and chemokines, such as TGF- β , IL-10, and CCL2, which hinder T cell activation and facilitate the recruitment of immunosuppressive cells to the TME. Furthermore, TAMs can impede T cell proliferation by releasing factors like indoleamine 2,3-dioxygenase (IDO) (57) and ARG1 (58), depleting essential nutrients necessary for T cell growth. Collectively, these mechanisms establish an immunosuppressive environment within the TME, enabling tumor cells to evade immune surveillance and promoting tumor growth and progression. Given their role in suppressing the immune system and limiting the efficacy of immune checkpoint inhibitors, TAMs have emerged as promising targets for cancer immunotherapy.

Various strategies have been developed to target TAMs in the TME. One approach involves suppressing the recruitment of TAMs into tumors by inhibiting specific molecules on TAMs, such as CCR2 and CCR5 (59, 60). Inhibiting these molecules or their ligands (CCL2 and CCL5) using inhibitors or antibodies can impede macrophage infiltration into tumors. Another

strategy is to decrease macrophage survival by inhibiting key signaling pathways that promote TAM survival and proliferation, such as the colony-stimulating factor 1 (CSF1)/CSF1 receptor (CSF1R) pathway (61). CSF1 inhibitors can impede the differentiation of monocytes into M2 macrophages and induce macrophage apoptosis, thus reducing the number of TAMs in the TME.

Inhibiting the tumor-promoting functions of TAMs is also a viable strategy. For example, blocking the Tim-3 receptor with antibodies has shown promise in regulating TAM activation (62). Additionally, anti-VEGF and anti-VEGFR agents can hinder the pro-tumoral functions of TAMs by inhibiting angiogenesis (63). Repolarizing TAMs from an M2-like immunosuppressive phenotype to an M1-like antitumor phenotype is another potential therapeutic strategy for cancer immunotherapy (64, 65).

Furthermore, the innate immune checkpoint molecule CD47, known as a "don't eat me" signal, is expressed on the surface of both normal and cancer cells (66). CD47 interacts with a macrophage receptor called signal-regulatory protein α (SIRP α), sending a signal to macrophages to avoid phagocytosing cells expressing CD47 (67). Overexpression of CD47 on cancer cells serves as a mechanism for immune evasion by preventing their phagocytosis by macrophages (68). Consequently, CD47 overexpression may indicate a reduced response to immune checkpoint inhibitors. Conversely, blocking the CD47/SIRP α interaction with anti-CD47 monoclonal antibodies could sensitize cancer cells to immune checkpoint inhibitors and potentially

enhance their response (69).

Macrophages have emerged as an attractive target in cancer immunotherapy due to their multifaceted roles in tumor growth, progression, and immune evasion. Consequently, TAMs provide an appealing target for the development of novel immunotherapeutic strategies against cancer.

1.4. The Thyroid Tumor Microenvironment

Thyroid cancer, the most common endocrine cancer, has experienced a rapid increase in incidence worldwide. It encompasses papillary thyroid cancer (PTC), follicular thyroid cancer (FTC), and anaplastic thyroid cancer (ATC). While differentiated thyroid cancers like PTC and FTC generally have favorable prognoses with 80-95% 10-year survival rates, ATC and a small percentage of thyroid cancers exhibit extremely poor survival rates (70, 71). Notably, the presence of the BRAF^{V600E} mutation in approximately 40-50% of PTC and ATC cases is associated with more aggressive tumor behavior and a worse prognosis (72, 73).

In the thyroid tumor microenvironment (TME), tumor-associated macrophages (TAMs) increase in high-grade thyroid cancer and are correlated with decreased cancer-related survival (56). Specifically, increased numbers of CD163⁺ and CD68⁺ cells, markers of TAMs, have been linked to poor overall survival in ATC (74), and high-density TAM infiltration is associated with larger tumor sizes compared to low-density infiltration (75). TAM-derived cytokines play a role in thyroid tumor progression. For example,

CXCL8, highly expressed in TAMs, acts as a chemoattractant for cancer cells and enhances invasion of PTC cells (76). Additionally, the co-culture of monocytes with PTC induces upregulation of CXCL16, resulting in PTC cell migration, enhanced angiogenesis, and tumor growth (77, 78). Thus, targeting cytokines secreted by TAMs may hold therapeutic potential in the TME of thyroid cancer.

1.5. Suggested oncogenic role of Collagen Type VI Alpha 3 in TME

The extracellular matrix (ECM) within the TME plays a critical role in regulating cancer progression and metastasis (79, 80). Comprising a complex network of proteins and carbohydrates, the ECM surrounds cells and provides structural support. Collagen, a major ECM component, can act as a signaling molecule, activating pathways that promote tumor cell survival and migration (81).

Collagen type VI alpha 3 (COL6A3) is a specific isoform of collagen type VI belonging to the family of ECM proteins. Collagen type VI consists of three alpha chains (alpha 1, alpha 2, and alpha 3) that form a triple helical structure (82). Among these chains, the alpha 3 chain is the longest and is associated with collagen type VI.

Especially, the cleaved C-terminal C5 domain of COL6A3 is referred to as endotrophin (ETP) (83). The α 3 chain, by far the longest of the three chains, contains an unusually long N terminus and a globular C5 domain at the C-

terminus. The C-terminal portion of the $\alpha 3$ subunit is cleaved off during the post-translational processing of COL6 fibrils and molecular weight of ETP is approximately 10–15 kDa. Recently, accumulating evidence has suggested that ETP plays oncogenic roles in tumor progression (83-85). Studies conducted on transgenic mice that overexpress ETP have demonstrated a significant rise in tumor volume and metastatic burden (83). Moreover, ETP has been found to induce epithelial-mesenchymal transition (EMT) in cells by activating the transforming growth factor-beta (TGF- β) signaling pathway, which consequently enhances cancer cell migration (83, 84). However, several crucial mechanisms pertaining to the biological process of ETP production in various human pathophysiologies and the oncogenic actions of ETPs in the human tumor microenvironment (TME) remain undetermined.

1.6. ECM Interactions in the Tumor Microenvironment of Advanced Thyroid Cancer

Among various human solid cancers, anaplastic thyroid carcinoma (ATC)/poorly differentiated thyroid carcinoma (PDTC) has been identified as a tumor type characterized by an extremely high abundance of macrophages, representing a "hot tumor" phenotype (86). Recent studies utilizing single-cell transcriptomics analysis have demonstrated that highly aggressive anaplastic transformation in ATC/PDTC is accompanied by excessive production of collagen, upregulation of collagen-interaction receptors, resulting in a mesenchymal change of epithelial cells, macrophage

polarization from M1 to M2 phenotype, and reprogramming of T cells from cytotoxic to exhausted cells. These findings emphasize the importance of studying the interactions between cancer cells and cells in the tumor microenvironment (TME), particularly regarding the extracellular matrix (ECM) components such as the active form of collagen, like ETP, in ATC/PDTC tumors. Furthermore, there is evidence of an association between COL6A3 expression and thyroid cancer, with significant upregulation observed in an aggressive subgroup of papillary thyroid carcinoma (PTC) patients (87). Moreover, COL6A3 was found to be overexpressed in the ATC/PDTC group compared to the PTC and follicular thyroid carcinoma (FTC) groups (88). These findings suggest a potential role of COL6A3 in the aggressive behavior of ATC/PDTC. In addition to the clinical evidence, I have developed a novel orthotopic syngeneic mouse model of ATC using mouse thyroid anaplastic thyroid cancer cells. This model closely mimics human ATC, exhibiting a "hot tumor" phenotype characterized by a high density of macrophages and other immune cells. As a result, this mouse model provides a valuable tool for studying the role of ETP in advanced thyroid cancer in a preclinical setting.

1.7. Aim of the study

This study aimed to investigate the oncogenic role of ETP in macrophage-enriched thyroid cancer tumor microenvironments.

In Part I, the origin of the ETP-secreting cells in the thyroid cancer microenvironment was investigated. The effect of ETP on BRAF^{V600E} thyroid cancer cells was also examined. This is helpful to understand the process of ETP production and its effects in the TME of thyroid cancer.

In Part II, differentially expressed genes were evaluated to determine the mechanism of the effect of ETP on BRAF^{V600E} thyroid cancer cells using RNA sequencing. The objective is to investigate gene alterations in thyroid cancer cells that are caused by ETP.

In Part III, the effect of the lack of ETP on thyroid tumor growth was explored *in vivo* using Col6a3-KO mice. Based on *in vitro* experiments, the goal is to observe the effect of ETP on tumor growth and the components of TME *in vivo*.

2. Materials and Methods

2.1. Animal experiments

Five-week-old female C57BL/6 mice were purchased from Orient Bio, Inc. (Sunghnam, South Korea) and housed in a pathogen-free facility. All the animals were maintained and used in accordance with the Guidelines for the Care and Use of Laboratory Animals of the Institute of Laboratory Animal Resources, Seoul National University.

Col6a3-KO mice [C57BL/6N-Col6a3^{em1(IMPC)KMPC/KMPC}] were a kind gift from Prof. Jiyoung Park (Department of Biological Sciences, College of Information and Bioengineering, Ulsan National Institute of Science and Technology, Ulsan, Republic of Korea).

An orthotopic tumor model was established by the intrathyroidal injection of tumor cells. For intrathyroidal injection, 1×10^5 TBP3743-B6 cells in 10 μ L of phosphate buffered saline (PBS, Gibco, New York, USA) were injected into the left thyroid gland of the mice using a Hamilton syringe with a 30G needle.

2.2. Cell culture

Human thyroid cancer cell lines, BCPAP cells as PTC, FRO cells as ATC, and the human monocyte cell line THP-1 were cultured in Roswell Park Memorial Institute (RPMI) 1640 medium (WELGENE, Seoul, Korea) containing 10% fetal bovine serum (FBS; WELGENE) and 1% penicillin

(100 unit/mL)/streptomycin (100 µg/mL; Gibco, New York, NY). The mouse anaplastic thyroid cancer cell line TBP3743-B6 was cultured in RPMI 1640 medium containing 10% FBS and 1% penicillin (100 U/mL)/streptomycin (100 µg/mL). THP-1 cells are a human leukemia monocytic cell line and a suitable *in vitro* cell model to study activity of macrophage functions (90), and phorbol 12-myristate 13-acetate (PMA) can be induced differentiation of THP-1 monocytes into macrophages (89). All cells were cultured at 37 °C in 5% CO₂ and 95% air.

2.3. Harvest of ETP conditioned medium

To collect the ETP-enriched CM, 293T cells were seeded on 100 mm culture dishes at 3×10^6 cells/mL in 10 mL of Dulbecco's Modified Eagle's medium (DMEM; WELGENE) supplemented with 10% FBS. For the transfection, the medium was changed to a serum-free medium, and 15 µg of pTRE-ETP plasmid was added to the lipofectamine transfection reagent 3000 (Thermo Fisher Scientific). The same amount of empty pTRE plasmid was used as a control medium. After 24 h, the medium was collected and centrifuged to remove the dead cells and debris. The medium was then validated for secreted ETP levels by western blot analysis.

2.4. Harvest of anti-ETP antibody medium

A rat hybridoma cell line expressing an anti-ETP monoclonal antibody

was seeded on 100 mm culture dishes at 3×10^6 cells/mL in 10 mL of DMEM supplemented with 10% FBS. After overnight incubation, the medium was changed to a serum-free medium and incubated for 24 h. The medium was then collected and centrifuged to remove dead cells and debris.

2.5. Preparation of conditioned medium

BCPAP and FRO cells were seeded in 100 mm culture dishes at a density of 3×10^6 cells/mL in 10 mL of RPMI 1640 medium supplemented with 10% FBS. The next day, the cells reached a >80% confluent monolayer, were washed once with PBS, and the medium was replaced with RPMI 1640. After 24 h, the conditioned medium (CM) was collected.

THP-1 cells were seeded in 100 mm culture dishes at a density of 6×10^6 cells/mL in 10 mL of RPMI 1640 medium supplemented with 10% FBS and 5 μ M PMA. The next day, cells were washed once with PBS, and the medium was replaced with RPMI 1640. After 24 h, the CM was collected.

To collect co-culture conditioned medium (CoCM), BCPAP or FRO cells were seeded on 100 mm culture dishes at 3×10^6 cells/mL in 10 mL of RPMI 1640 medium supplemented with 10% FBS. The next day, the cells reached a >80% confluent monolayer, were washed once with PBS, and THP-1 cells were seeded at 6×10^6 cells/mL in 10 mL of RPMI 1640 medium supplemented with 10% FBS and 5 μ M PMA and incubated for 24 h. The following day, the cells were washed once with PBS, and the medium was

replaced with RPMI 1640 medium. CoCM was collected 1 day after confluence.

2.6. Immunohistochemistry staining

Formalin-fixed, paraffin-embedded human thyroid tissues were evaluated using anti-ETP and mouse thyroid tumor tissues were evaluated using anti-ETP, anti-CD8, anti-CD4, and anti-CD163 antibodies. Paraffin sections were deparaffinized in Histo-Clear (National Diagnostics, Atlanta, GA, USA) and rehydrated by gradually reducing the ethanol concentration from 100% to 95% and then to 90%. Antigen epitopes were then unmasked using Tris-EDTA buffer (pH 9.0). Subsequently, the slides were incubated at 4°C with the primary antibodies. After overnight incubation, the slides were incubated with horseradish peroxidase-conjugated secondary antibodies, followed by incubation with diaminobenzidine (DAB) solution for 10 min.

2.7. Immunofluorescent staining

Formalin-fixed, paraffin-embedded mouse thyroid tumor tissues were evaluated using anti-CD163, anti-ETP, and DAPI (nuclear staining) antibodies. Paraffin sections were deparaffinized in Histo-Clear and rehydrated by gradually reducing the ethanol concentration from 100% to 95% and then to 90%. Antigen epitopes were then unmasked using Tris-EDTA buffer (pH 9.0). Subsequently, the slides were incubated at 4°C with the primary antibodies. After overnight incubation, the slides were incubated with

fluorescent-conjugated secondary antibodies.

2.8. Real-time PCR analysis

Total RNA from cultured cells or *in vivo* orthotopic tumors was extracted using TRIzol Reagent (Invitrogen, San Diego, CA, USA), and 1 µg RNA was used to synthesize cDNA using the MMLV Reverse Transcriptase kit (Invitrogen). Realtime polymerase chain reaction (PCR) was performed using the StepOne Plus PCR system (Applied Biosystems, Foster City, CA) and TB Green Premix (Takara Bio Inc., Otsu, Japan) according to the manufacturer's protocol. The detailed primer sequences are listed in the Supplementary Data (Table 1).

2.9. Western blotting analysis

BCPAP or FRO cells were seeded on 100 mm culture dishes at 3×10^6 cells/mL in 10 mL of RPMI 1640 medium supplemented with 10% FBS. The next day, the cells reached a >80% confluent monolayer, were washed once with PBS, and THP-1 cells were seeded at 6×10^6 cells/mL in 10 mL of RPMI 1640 medium supplemented with 10% FBS and 5 µM PMA and incubated for 24 h. The following day, the cells were washed once with PBS, and the medium was replaced with RPMI 1640 medium. CoCM was collected 1 day after confluence.

The cell culture medium was collected and concentrated using an Amicon 3k centrifugal filter (Millipore Merck, Darmstadt, Germany)

following the manufacturer's instructions. The protein concentrations in the concentrated cell culture medium were measured using a Pierce™ BCA Protein Assay Kit (Thermo Fisher Scientific, MA, USA). The protein in the cell culture medium was separated using 15% sodium dodecyl sulfate polyacrylamide gels for electrophoresis and transferred to polyvinylidene fluoride membranes (PVDF; Bio-Rad, Hercules, CA, USA). The blotted PVDF membrane was first blocked with 5% milk for 1 h and then incubated with primary and secondary antibodies for 24 and 1 h, respectively. Further, membranes were developed using Super Signal™ West Pico PLUS Chemiluminescent Substrate (Thermo Fisher Scientific).

2.10. Cell migration assay

Cell migration was assessed using a transwell system (Corning, NY, USA). An 8 µm pore-size polycarbonate membrane was coated with 0.2% gelatin solution for 1 h and then dried overnight. The upper chamber contained 1×10^5 cells in a 24-well plate, while the lower chamber was filled with 650 µL media. After 12 h, the non-migrating cells were swabbed with a cotton-tipped applicator, fixed in methanol for 30 min, and stained with 1% crystal violet for 30 min.

2.11. Cell viability assay

For the cell viability study, cells were seeded in a 96-well tissue culture plate with 100 µL of medium at 8×10^3 cells/mL. After culturing for 1 d, the

cells were rinsed with PBS and treated with ETP-CM at the indicated times, and a CCK-8 assay was performed (Dojindo, Kumamoto, Japan). CCK-8 solution (10 μ L) was added to each well, and after a 2-h incubation, the absorbance at 450 nm was measured using a microplate reader (SpectraMax 190; Molecular Devices, San Jose, CA).

2.12. Isolation of bone marrow-derived monocytes/macrophages

Bone marrow-derived monocytes/macrophages (BMMs) were isolated from the mice by flushing with minimum essential medium (MEM, Gibco) containing penicillin (100 units/mL) and streptomycin (100 g/mL). The cells were filtered through a 70 μ m nylon filter, centrifuged for 5 min at 550 g, and then plated in a 90 \times 15 mm Petri dish at 3×10^6 cells in α -MEM medium containing 10% FBS and 1% penicillin (100 unit/mL)/streptomycin (100 g/mL) with macrophage colony-stimulating factor (M-CSF, 30 ng/mL; R&D Systems, Minneapolis, MN, USA). One day later, attached BMMs were harvested by scraping.

To collect the BMM CoCM, FRO cells were seeded in 100 mm culture dishes at 3×10^6 cells/mL in 10 mL of RPMI 1640 medium supplemented with 10% FBS. The next day, the cells reached a >80% confluent monolayer, were washed once with PBS, and WT or Col6a3-KO BMMs were seeded at 9×10^6 cells/mL in 10 mL of RPMI 1640 medium supplemented with 10% FBS and 30 ng/mL M-CSF and incubated for 24 h. The next day, the cells

were washed once with PBS, and the medium was replaced with RPMI 1640 medium. BMM CoCMs were collected one day before confluence.

2.13. RNA sequencing

FRO cells were treated with FRO single CM (FRO-sCM), FRO with WT mice BMM co-culture CM (FRO/WT-coCM) or FRO with Col6a3-KO mice BMM co-culture CM (FRO/KO-coCM) for 4 h, and total RNA was extracted using the TRIzol Reagent. Total RNA was used to construct cDNA libraries using the TruSeq stranded RNA library kit (Illumina, San Diego, CA, USA) according to the manufacturer's instructions. Sequencing was performed using an Illumina HiSeq2000 (Illumina) platform with approximately 100 nt paired-end reads. The quality of the raw sequence data was assessed using FastQC (FastQC 0.11.7). Subsequently, sequenced reads were aligned to the mm10 mouse genome assembly (GRCh37) reference genome using the HISAT2 aligner (HISAT2 2.1.0). Raw read counts were used to analyze the differentially expressed genes (DEGs) among the groups using the Cuffdiff workflow (Cuffdiff 2.2.1). DEGs were defined as genes with a false discovery rate (FDR) < 0.05 and an absolute log₂ fold change >1.

2.14. Statistical analysis

All experiments were performed at least thrice. Data are expressed as mean ± standard deviation. Statistical analyses were performed using GraphPad Prism software version 9 with the t-test and analysis of variance

(ANOVA). Statistical significance was set at $p < 0.05$.

Table 1. Primer sequences

Gene	Forward primer	Reverse primer
<i>COL6A3</i>	CAGCTGTCCTGGCTCAAAAA	ACATAGCCCACACCGTTCTC
<i>MMP9</i>	TTGACAGCGACAAGAAGTGG	GCCATTCACGTCGTCCTTAT
<i>MMP14</i>	ACCTACGTACCCACACACAG	TGCCATTTGAGACCCTGGAT
<i>MMP11</i>	CTCGTGGGTCCTGACTTCTT	GCAGTTGTCATGGTGGTTGT
<i>MMP13</i>	TTCAAGATGCATCCAGGGGT	CCAGTCACCTCTAAGCCGAA
<i>MMP15</i>	TGGGGCAGGGTGTTTAGAAT	TCCTAAGGCCCAGAGAGACT
<i>MMP16</i>	ACTGACAGAGCCAAGAGACC	TCTGACTCATGGGGTGCATT
<i>GAPDH</i>	ATGGGGAAGGTGAAGGTCGG	GACGGTGCCATGGAATTTGC
<i>Cd247 (Cd3)</i>	GATGCGGTGGAACACTTTCT	ACTGTCCTCGACTTCCGAGA
<i>Cd4</i>	AGGAAGTGAACCTGGTGGTG	TCCTGGAGTCCATCTTGACC
<i>Cd8a</i>	GCGGTACGGTAAATCTGGAA	TCAGATTCAACGCCTCTCCT
<i>Adgre1 (F4/80)</i>	CTTTGGCTATGGGCTTCCAGTC	GCAAGGAGGACAGAGTTTATC
<i>Cd69</i>	TTTGGAGGGGTTTCAGTGGT	GCTGTCTACACGGAGGAAGT
<i>Cd161</i>	ATCTCCAGTCTCTGCCCATG	TGAATGCCCATACCCCTTGT
<i>Cd80</i>	AGTTGGAGGCACAGTTCGTA	GCAAAAGCCACTTCCAGGAA
<i>Cxcl10</i>	GCCGTCATTTTCTGCCTCAT	GATAGGCTCGCAGGGATGAT
<i>Cd206</i>	TGGATGGATGGGAGCAAAGT	GCTGCTGTTATGTCTCTGGC
<i>Arg1</i>	CTGAGCTTTGATGTCGACGG	TCCTCTGCTGTCTTCCCAAG
<i>Gapdh</i>	CCAGAACATCATCCCTGCATC	GGTCCTCAGTGTAGCCCAAGAT

3. Results

3.1. Expression and Association of Endotrophin and CD163-positive TAM in Human Thyroid Cancer Tissues

To gain insight into the expression of ETP in the tumor microenvironment of thyroid cancer, I conducted immunohistochemical staining on a diverse range of human thyroid tissues, including normal thyroid (n=7), autoimmune thyroid disease (AITD, n=45), benign adenoma (n=57), and both PTC (n=263) and ATC (n=17). ETP expression was detected in a subset of papillary thyroid carcinoma (PTC) tissues and all anaplastic thyroid carcinoma (ATC) tissues, while it was not observed in normal thyroid, benign adenoma, or AITD (Table 2 and Figure 1A). In thyroid cancer tissues, ETP expressions were predominantly observed in the stromal regions (Figure 2A) and areas with fibrosis (Figure 2B), indicating a stromal-dominant pattern of ETP expression. Among all thyroid cancer tissues, quantification of ETP-positive area % were divided into 4 groups based on quartile values. ETP expressions were significantly higher in ATC tissues compared to PTC tissues, as evidenced by both the quantification of ETP-positive area percentages in the highest quartile group (Q4: 88.2 [ATC] vs 21.3 [PTC] %, $P < 0.001$, Figure 1B), and the mean ETP-positive area % (38.2 ± 25.4 vs 10.9 ± 12.1 %, $P < 0.001$, Figure 1B).

To further investigate the clinicopathological characteristics of thyroid

cancer patients based on ETP expression, all PTC patients were categorized into two groups using the median value of ETP-positive area (7.75 %) as the cutoff. These groups were designated as the ETP-low and ETP-high groups. The mean diagnostic age and sex ratio did not differ significantly between the two groups, while the ETP-high group exhibited a higher body mass index compared to the ETP-low group (25.5 ± 4.8 vs 24.7 ± 3.3 kg/m², $P=0.048$, Table 3). Additionally, the ETP-high group showed significantly larger primary tumor size (1.59 ± 0.98 vs 2.17 ± 1.31 , $P<0.001$, Table 3), and a higher incidence of lymph node metastasis (45.2 vs 33.1 %, $P=0.044$, Table 3) in ETP-high group compared to ETP-low group, suggesting that higher ETP expression in human PTCs is associated with pathologically aggressive features.

Next, based on the two findings mentioned, the association between ETP expressions and TAM densities was investigated. First, higher ETP expression in human PTCs is associated with pathologically aggressive features. Second, ETP expressions are significantly higher in ATC compared to PTC. Considering that TAM densities are established poor prognostic factors in PTCs (75), and ATC is recognized as a TAM-enriched tumor with extremely poor survival, further exploring the relationship between ETP expressions and TAM densities becomes essential. Among all enrolled tissues, 260 of PTC and 14 of ATC tissues were stained with anti-CD163 as representative marker for TAM (86). Consistent with previous reports (77), the quantification of CD163-positive area percentages revealed a significant

increase in ATC tissues compared to PTC tissue (48.6 ± 10.8 vs 14.6 ± 8.7 %, $p < 0.001$, Figure 1C). Conversely, adjacent normal tissue exhibited no expression of CD163. Additionally, a positive correlation was observed between ETP expression and CD163 expression in tumor tissues ($r^2 = 0.238$, $p < 0.001$, Figure 1D). Collectively, ETP exhibited cancer-specific, stromal-dominant expression in human thyroid tumor tissues and showed a positive correlation with TAM density. Based on these findings, it is reasonable to hypothesize that TAMs play a crucial role as one of the essential components in the production and action of ETP in the tumor microenvironment of patients with advanced TAM-enriched thyroid cancer.

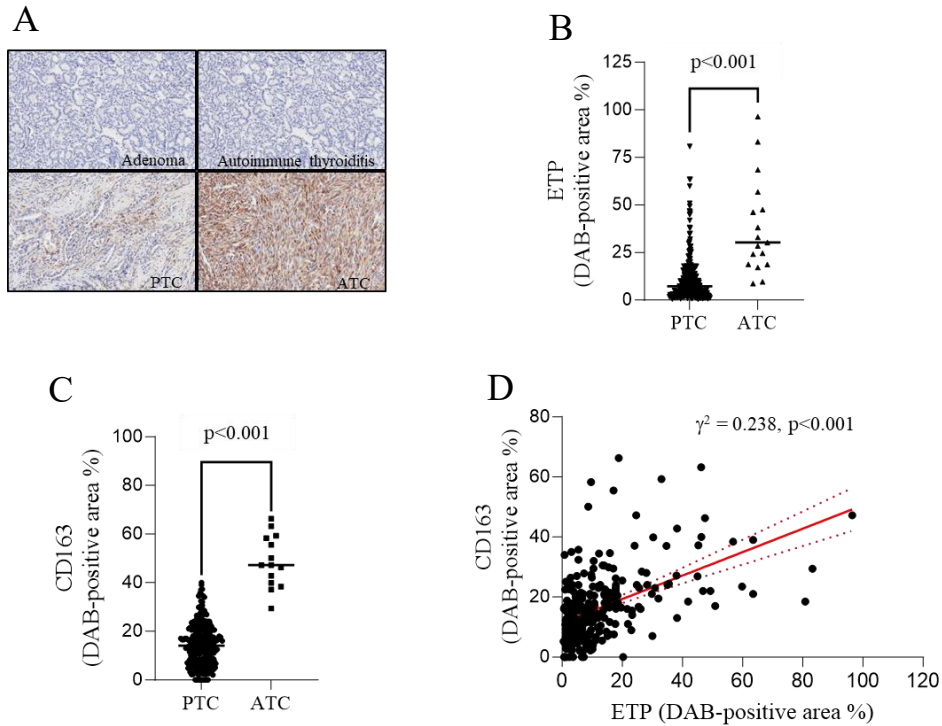


Figure 1. Expression of ETP in various types of human thyroid tissue.

Immunohistochemical (IHC) staining was performed in A. thyroid disease tissues or cancer tissues and B. PTC or ATC tissues with anti-ETP antibody. B. Expression of ETP in PTC and ATC, respectively. C. Expression of CD163 in PTC and ATC, respectively. D. Correlation between CD163⁺ macrophage and ETP was analyzed by IHC staining. ETP, endotrophin; PTC, papillary thyroid cancer; ATC, anaplastic thyroid cancer.

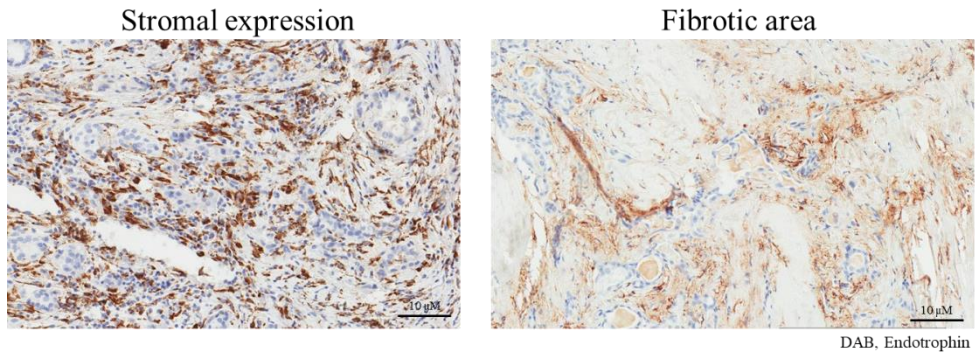


Figure 2. Regions of ETP-expressed in thyroid cancer tissues.

Immunohistochemical (IHC) staining was performed in thyroid cancer.

Expression of ETP in the stromal regions and areas with fibrosis.

Table 2. Immunohistochemical staining of ETP in various human thyroid tissues.

Thyroid disease		Normal	AITD	Adenoma	PTC	ATC	¹ P-value
Number of patients		7	45	57	263	17	
² ETP expression (area %)	Q1 (0.5-3.2)	7 (100)	45 (100)	57 (100)	67 (25.5)	–	<0.001
	Q2 (3.2-7.8)	–	–	–	73 (27.7)	–	
	Q3 (7.8-15.7)	–	–	–	67 (25.5)	2 (11.8)	
	Q4 (≥ 15.7)	–	–	–	56 (21.3)	15 (88.2)	

¹P-value from Chi-square between two groups, PTC and ATC. ²The ETP-positive area percentages were divided into four groups based on quartile values. AITD, autoimmune thyroid disease; PTC, papillary thyroid cancer; ATC, anaplastic thyroid cancer

Table 3. Clinical characteristics of patients with thyroid cancer patients based on ETP expression

ETP expression	Low (n=64)	High (n=52)	P-value
Age at diagnosis, yr	51.7 ± 12.0	50.3 ± 13.2	0.169
Sex, female, n (%)	50 (78.1)	42 (78.1)	
Body mass index, kg/m ²	24.7 ± 3.3	25.5 ± 4.8	0.048
Tumor size, cm	0.8 ± 0.3	1.4 ± 0.8	<0.001
Multifocality, n (%)	21 (32.8)	30 (57.7)	0.013
Extrathyroidal extension, n (%)	41 (64.1)	45 (86.5)	0.005
Lymphatic invasion, n (%)	12 (18.8)	19 (36.5)	0.031
Vascular invasion, n (%)	3 (4.7)	4 (7.7)	0.500
LN metastasis, n (%)			
Central neck	25 (39.1)	31 (59.6)	<0.001
Lateral neck	2 (3.1)	12 (23.1)	<0.001
LN meta ratio, n (%)			
Central neck	0.2 ± 0.3	0.3 ± 0.3	<0.001
Lateral neck	0.0 ± 0.1	0.1 ± 0.2	<0.001
SUV _{max} on FDG-PET			
Tumor	2.7 ± 1.6	6.5 ± 7.1	<0.001
Thyroid	1.5 ± 0.5	1.7 ± 1.3	0.069
Tumor/Thyroid	1.9 ± 1.3	4.5 ± 5.3	<0.001

3.2. Peritumoral Co-localization of Endotrophin Expressions with CD163-Positive Macrophage Concentration: Evidence from a Syngeneic Mouse Model of ATC

To investigate the further evidence of ETP production from TAMs in thyroid cancer microenvironments, newly generated orthotopic syngeneic mouse model were used (130).

A thyroid cancer mouse model was generated by orthotopic injection of TBP3743-B6 cells into the thyroids of C57BL/6 mice (Figure 1). The TBP3743 murine ATC cell line generated from B6129SF1 hybrid mice with a thyroid-specific *Braf*^{V600E} mutation (90). Additionally, TBP3743 cells were adapted into C57BL/6 inbred mice via *in vivo* passaging and established a novel orthotopic tumor model of ATC. Adapted TBP3743 cells were named as TBP3743-B6 cells.

Immunohistochemical (IHC) staining of tumor sections revealed a concentration of CD163⁺ macrophages in the peritumoral area, while CD4⁺ and CD8⁺ T cells were predominantly clustered in the central region. Remarkably, a correlation was observed between ETP expressions and the concentration of CD163⁺ macrophages in the peritumoral area (Figure 3). Furthermore, the co-localization of CD163⁺ and ETP⁺ in macrophages was further validated through immunofluorescence (IF) staining (Figure 4). These findings indicate that ETP is predominantly expressed in M2 macrophages that are enriched in the peritumoral area in ATCs.

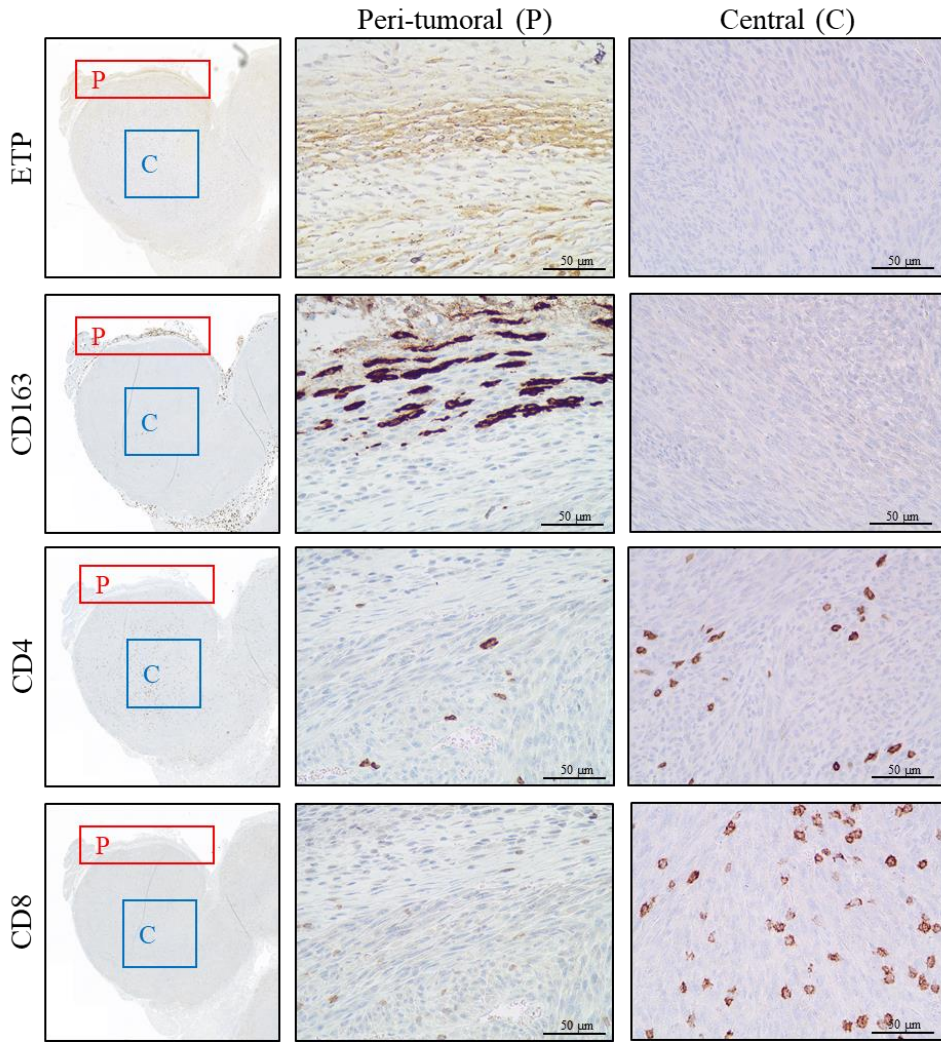


Figure 3. Expression of ETP in macrophage-enriched thyroid TME.

C57BL/6 mice were implanted with 10^5 cells of TBP3743-B6. Fourteen days post-implantation, the tumors were harvested. Representative images of IHC for ETP, M2-macrophage (CD163), helper T cells (CD4), and cytotoxic T cells (CD8) in tumors. ETP, endotrophin; IHC, immunohistochemistry.

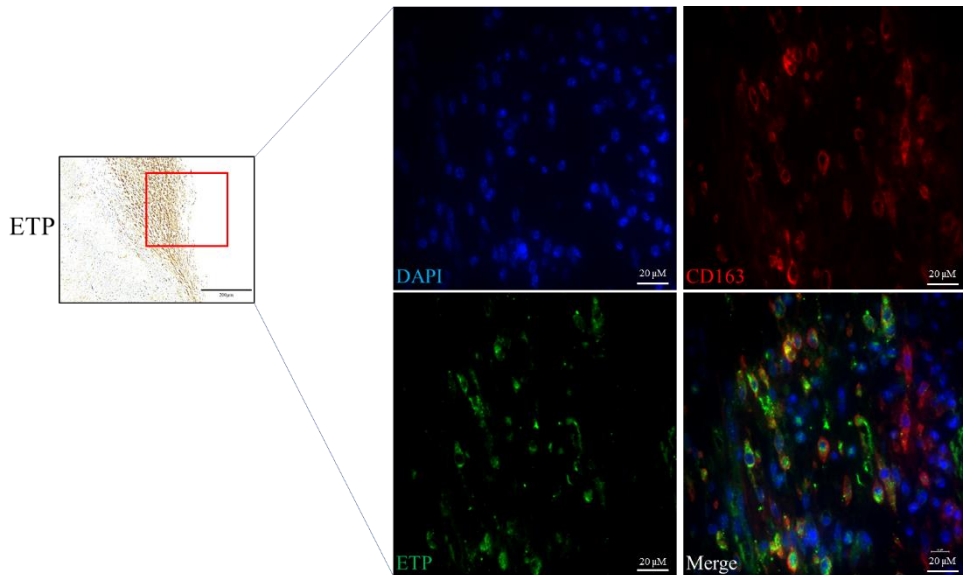


Figure 3. Co-localization of ETP expression and M2-macrophages in the TME of thyroid cancer.

C57BL/6 mice were implanted with 10^5 cells of TBP3743-B6. Fourteen days post-implantation, the tumors were harvested. Representative images of IF for M2-macrophage (CD163) and ETP in tumors. ETP, endotrophin; IF, immunofluorescence.

3.3. Enhanced ETP Production from Macrophages via Thyroid Cancer Cells-Macrophage Interactions

To investigate the production of ETP at the cellular level, THP-1 cells were treated with FRO-CM or BCPAP-CM for 24 hours, and the expression of *COL6A3* was measured using RT-qPCR. The results showed a significant upregulation of *COL6A3* expression in the groups treated with FRO-CM or BCPAP-CM compared to the control group (Figure 5A). Conversely, the expression of *COL6A3* in the cancer cells, per se, was negligible and did not show any significant upregulation upon treatment with CM from THP-1 single cultures (Figure 5B). These findings collectively indicate that *COL6A3* expression is upregulated in macrophages upon stimulation by factors derived from cancer cells *in vitro*.

Subsequently, the production of ETP protein was investigated in a co-culture system involving macrophages and cancer cells, aiming to mimic the tumor microenvironment (TME). Western blot analysis revealed a significant increase in secretory ETP levels in the medium of co-cultures of THP-1 cells with FRO or BCPAP cells compared to that in the medium of THP-1 single cultures (Figure 6). These findings collectively demonstrate that macrophage-derived ETP is enhanced through interactions with cancer cells within the TME of thyroid cancer.

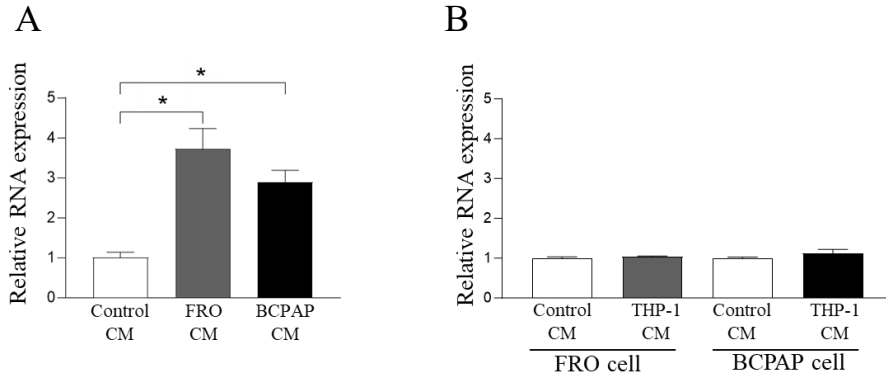


Figure 5. Upregulation of *COL6A3* gene in THP-1 cells by thyroid cancer cell CM.

A. THP-1 cells were cultured with FRO- or BCPAP-CM for 24 h, respectively, and the expression of *COL6A3* was analyzed by RT-qPCR. B. FRO or BCPAP cells were cultured with THP-CM for 24 h, respectively, and the expression of *COL6A3* was analyzed by RT-qPCR. Data are presented as mean \pm SD. * $p < 0.05$.

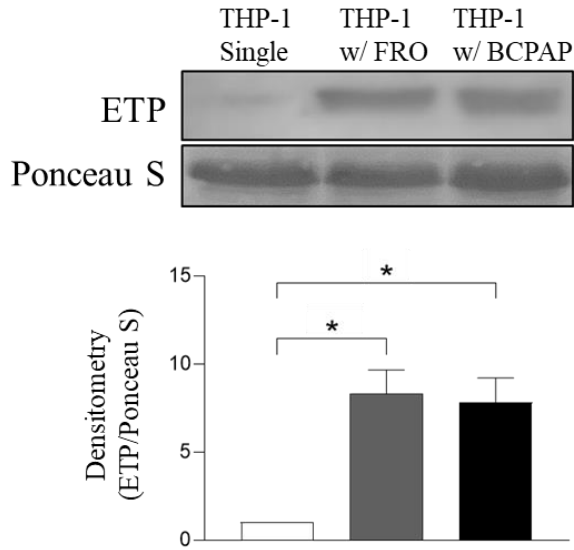


Figure 6. Macrophage-derived ETP *in vitro*.

THP-1 cells were co-cultured with FRO or BCPAP cells for 24 h and the co-cultured medium was harvested. The secreted ETP in the co-cultured medium was analyzed using western blot. Data are presented as mean \pm SD. * $p < 0.05$.

ETP, endotrophin.

3.4. The effects of ETP on Cell Viability in Thyroid Cancer Cells

Next, the effects of ETP on cancer cells were investigated. Firstly, a CCK-8 assay was performed to assess the impact of ETP on cancer cell viability. FRO or BCPAP cells were treated with ETP-conditioned medium (ETP-CM, 50%) for 24 or 48 hours. The results of the CCK-8 assay indicated that ETP had no significant effect on the viability of thyroid cancer cells at either time point (Figure 7).

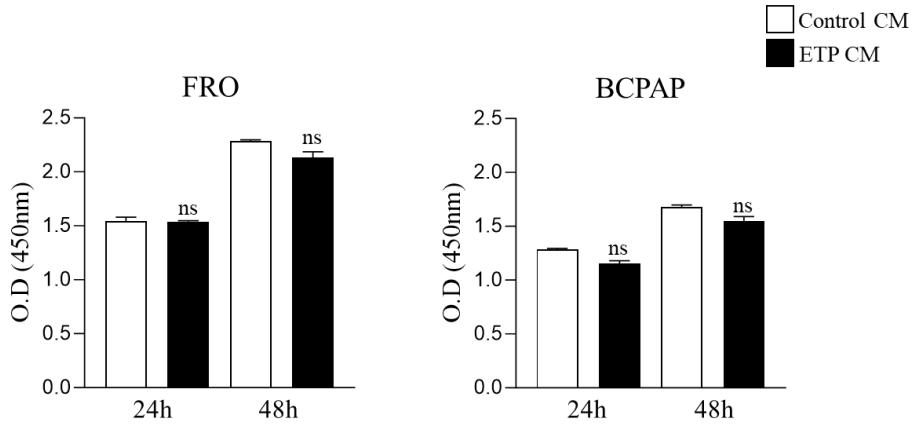


Figure 7. ETP effects on thyroid cancer cell proliferation.

FRO and BCPAP cells were treated with ETP-CM for the indicated times, and cell viability was measured using the CCK-8 assay. Data are presented as the mean \pm SD. ETP, endotrophin.

3.5. The Effects of ETP on Thyroid Cancer Cell Migration

To explore the effects of ETP on thyroid cancer cells, a cell migration study was performed on FRO and BCPAP cells using a Transwell migration system. First, treatment with ETP-CM (50%) significantly enhanced the migration potential of FRO or BCPAP cells compared with the control, and this effect was abolished by treatment with anti-ETP blocking antibody (Figure 8). Next, to validate these positive effects of ETP on cell migration potentials, CMs of co-cultures of THP-1 cells and FRO or BCPAP cells were used. As expectedly, both FRO-coCM and BCPAP-coCM significantly increased cancer cell migration potentials in FRO and BCPAP cells, respectively, whereas treatment with anti-ETP blocking antibody reduced it (Figure 9). Additionally, primary cultured bone marrow-derived macrophages (BMMs) from Col6a3-WT and Col6a3-KO mice were co-cultured with FRO or BCPAP cells, and conditioned media (CMs) were collected. Consistently, treatment with FRO/KO-coCM or BCPAP/KO-coCM significantly reduced the migration potential of the respective cancer cells compared to treatment with FRO/WT-coCM or BCPAP/WT-coCM (Figure 10).

Next, the impact of ETP on normal thyroid cells was evaluated. Htori cells, which are human normal thyroid epithelial cells immortalized through SV40 transfection (91), were used for the experiment. Notably, treatment with ETP-CM (50%) did not induce migration potential in Htori cells after 6 or 12 hours of treatment (Figure 11). These findings suggest that macrophage-

derived ETP specifically induces thyroid cancer cell migration potential, while its effect on cell migration is absent in normal thyroid cells.

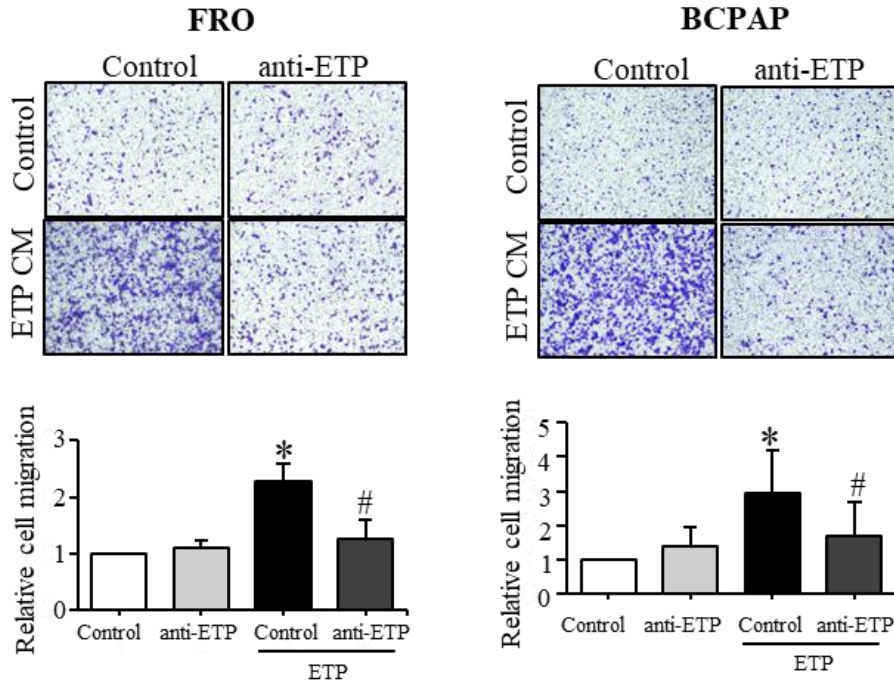


Figure 8. ETP supports the migration potentials of thyroid cancer cells.

Cell migration assays were performed using the Transwell system. FRO or BCPAP cells (10^5 cells/well) were inserted in the upper chambers and incubated in the presence of ETP-CM and/or anti-ETP specific blocking antibody in the bottom chamber for 12 or 6 h, respectively. Data are presented as mean \pm SD. * $p < 0.05$ versus control. # $p < 0.05$ versus ETP(+). ETP, endotrophin.

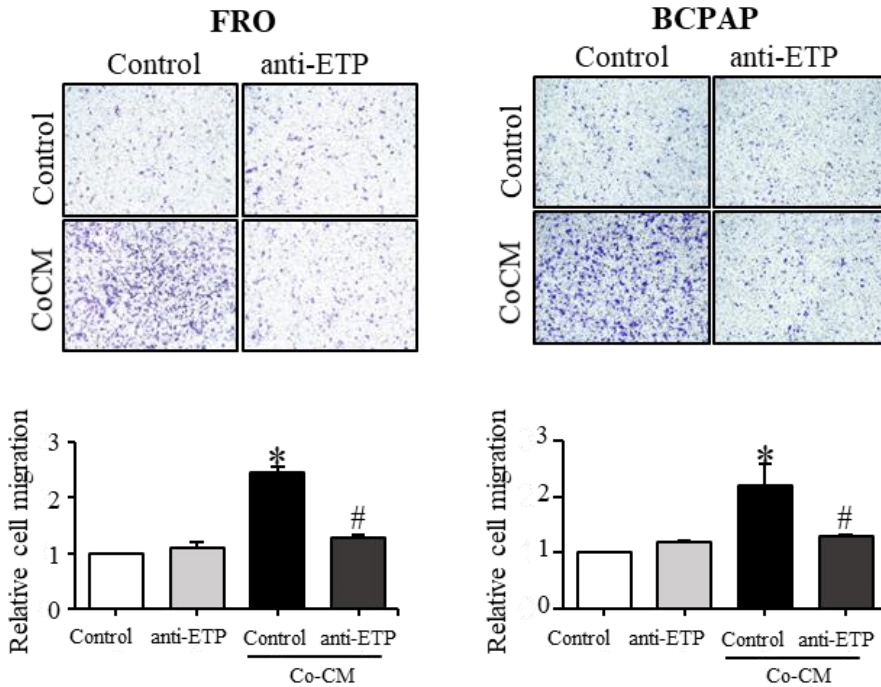


Figure 9. Macrophage-derived ETP supports the migration potentials of thyroid cancer cells.

Cell migration assays were performed using the Transwell system. FRO or BCPAP cells (10^5 cells/well) were placed in the upper chambers and incubated with CoCM and/or anti-ETP specific blocking antibodies in the bottom chamber for 12 or 6 h, respectively. Data are presented as mean \pm SD.

* $p < 0.05$ versus control. # $p < 0.05$ versus CoCM(+). ETP, endotrophin; CoCM, co-culture conditioned medium.

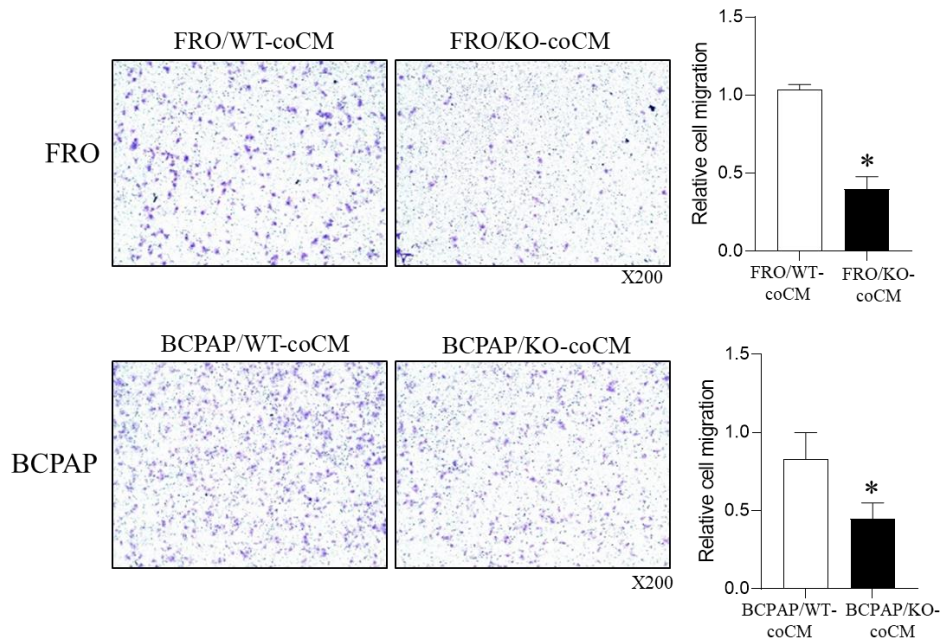


Figure 10. Col6a3-KO mice bone marrow monocytes coCM reduces the migration potentials of thyroid cancer cells.

FRO or BCPAP cells (10^5 cells/well) were inserted in upper chambers and incubated in the presence of BMM CoCM for 12 or 6 h, respectively. Data are presented as mean \pm SD. * $p < 0.05$ versus WT-CoCM. CoCM, co-culture conditioned medium.

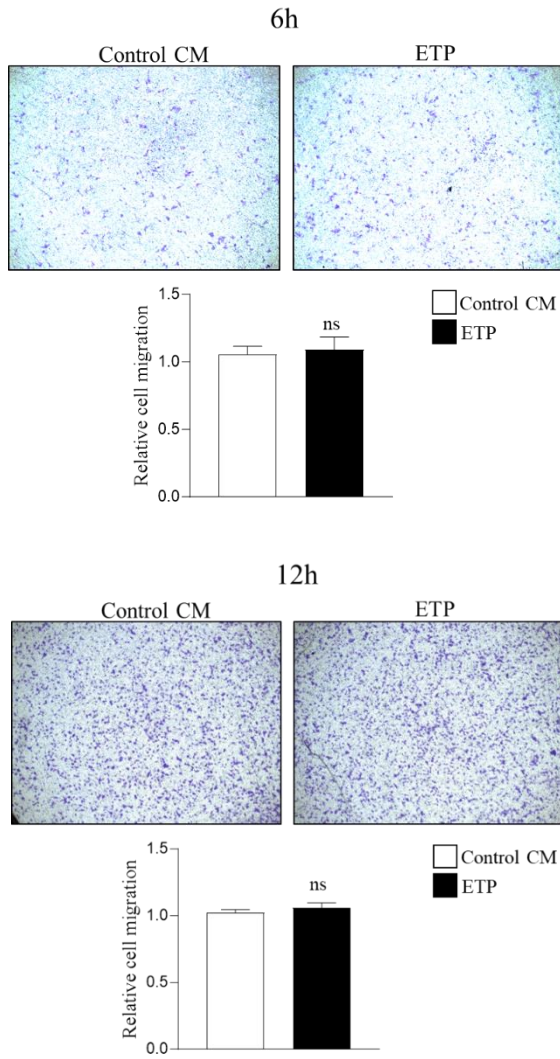


Figure 11. ETP has no effect of normal thyroid cell migration potential.

Cell migration assays were performed using the Transwell system. Htori cells (10^5 cells/well) were inserted in the upper chambers and incubated in the presence of ETP-CM or Control-CM in the bottom chamber for 6 and 12 h, respectively.

3.6. Molecular Mechanism of ETP-Mediated Cancer Cell Migration: Insight from transcriptomic analysis

To elucidate the molecular mechanisms underlying the effects of ETP on thyroid cancer cell migration, RNA sequencing analyses were conducted on total RNA isolated from FRO cells treated with FRO-sCM, FRO/WT-coCM or FRO/KO-coCM (n=3 for each group). Gene set enrichment analysis revealed a significant upregulation of gene sets associated with epithelial-mesenchymal transition (EMT, M5930) in FRO/WT-coCM-treated FRO cells compared to FRO-sCM-treated FRO cells, and this effect was markedly diminished in cells treated with FRO/KO-coCM. Notably, the expression of *SNAI2* and *FIBRONECTIN 1*, which are representative genes associated with EMT, exhibited a similar trend of change as observed in the overall gene set analysis, further supporting the involvement of EMT-related processes (Figure 12).

Furthermore, gene set enrichment analysis was performed on gene sets related to cell migration (GO:0090136, 0010634, 0010632). Among the intersecting genes, 8 genes, including *PTGS2*, *MMP9*, *RHOB*, *LGDN*, *VEGFA*, *SPARC*, *ABL1*, and *FGFR1*, were found to be significantly upregulated in FRO/WT-coCM-treated FRO cells compared to FRO-sCM-treated FRO cells. This effect was rescued in cells treated with FRO/KO-coCM, indicating the involvement of ETP in the regulation of these genes and their impact on cell migration (Figure 13).

Additionally, Pathway analysis revealed a significant upregulation of gene sets associated with JAK-STAT and TGF- β signaling pathways in FRO cells treated with FRO/WT-coCM compared to FRO cells treated with FRO-sCM. These pathways are well-known for their impact on cell migration potentials of various human cancers (92, 93), including thyroid (94). Importantly, the upregulation of these gene sets was not observed in cells treated with co-culture conditioned medium from FRO/KO BMMs (FRO/KO-coCM), indicating that the presence of ETP is necessary for their activation (Figure 14).

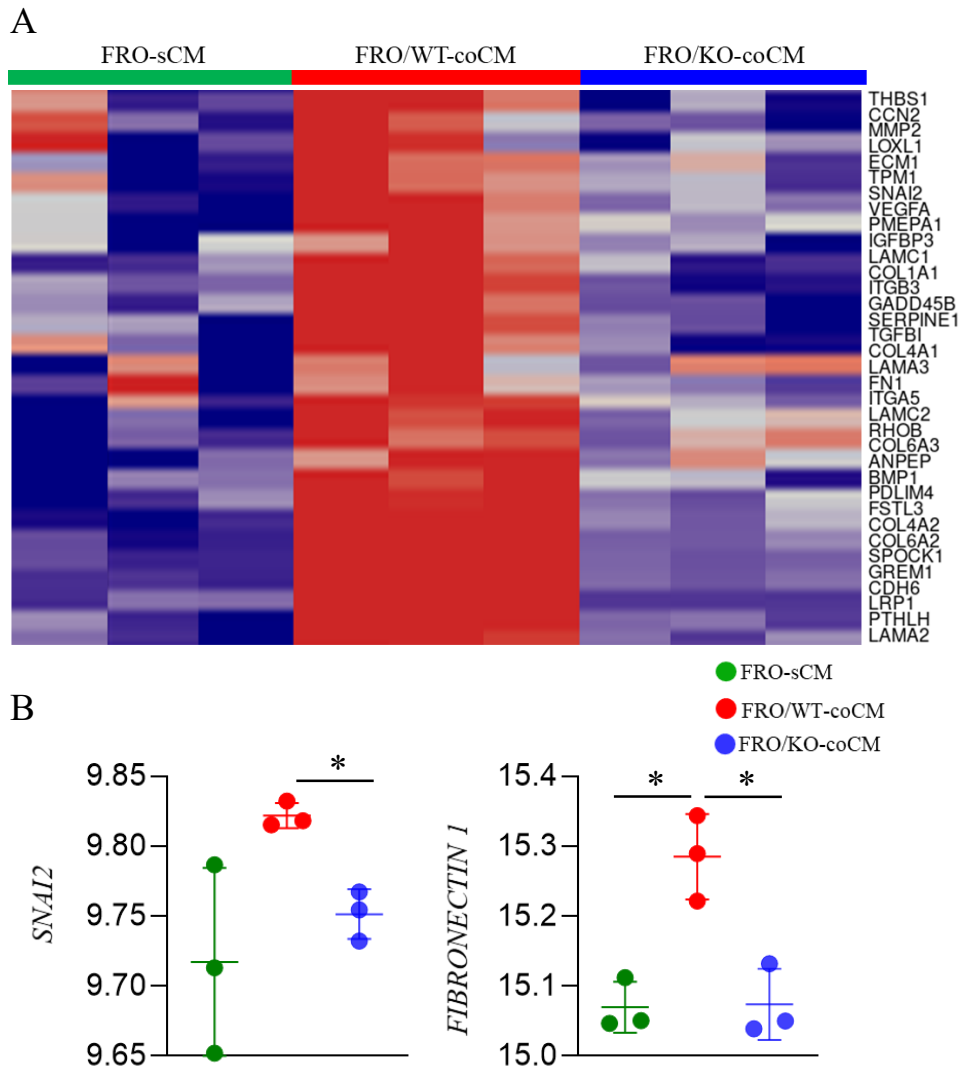


Figure 12. Molecular characteristics in epithelial mesenchymal transition related genes by RNA-sequencing.

FRO cells were incubated in the presence of FRO-sCM, FRO/WT-coCM or FRO/KO-coCM for 4 h. A. Heatmap was generated after a comparative analysis of FRO-sCM vs FRO/WT-coCM vs FRO/KO-coCM. Fold change > 2 and p-value < 0.1. B. change of epithelial mesenchymal transition related genes in FRO cells. *p < 0.05.

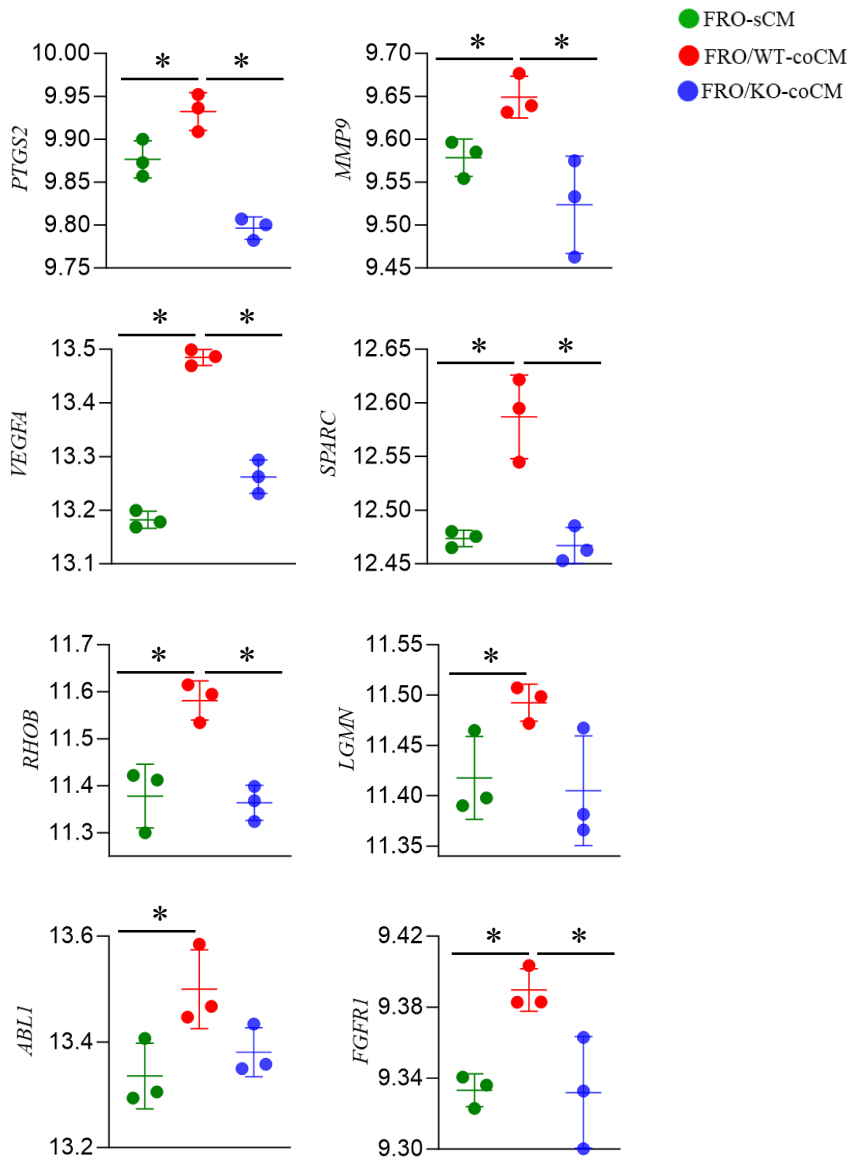


Figure 13. Expression of cell migration related genes in coCM-treated FRO cells.

FRO cells were incubated in the presence of FRO-sCM, FRO/WT-coCM or FRO/KO-coCM for 4 h. Alteration of cell migration related markers in FRO cells. * $p < 0.05$.

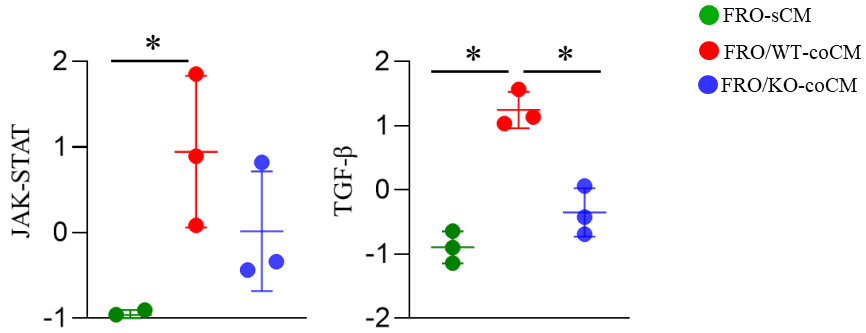


Figure 14. Analysis of oncogenic signaling pathways.

FRO cells were incubated in the presence of FRO-sCM, FRO/WT-coCM or FRO/KO-coCM for 4 h. Alteration of oncogenic pathways in FRO cells. *p < 0.05.

3.7. Comparing Tumor Growth and Microenvironments in an Orthotopic Syngeneic Animal Model using COL6A3-Deficient Mice

To investigate the oncogenic effects of ETP on tumor microenvironments *in vivo*, an orthotopic syngeneic model of thyroid cancer was developed using Col6a3-KO or WT mice. The model involved the intrathyroidal injection of the mouse ATC cell line TBP3743-B6. After a 2-week period, a significant reduction in both mean tumor volume (43% decrease) and tumor weight (46% decrease) was observed in the Col6a3-KO mice compared to the WT mice (Figure 15). Considering the absence of direct effects of ETP on cell viability *in vitro* (Figure 7), it led to the hypothesis that the differential tumor growth could be attributed to distinct microenvironments, involving immune reactions and angiogenesis. To investigate this further, immunohistochemical staining was conducted to compare the alterations in the tumor microenvironment between the two experimental groups. Both lymphoid and myeloid cells were analyzed, and among them, the most prominent increase was observed in cytotoxic CD8⁺ T cells. The fractional area of CD8⁺ T cells was significantly increased in the tumors from Col6a3-KO mice compared to that in the WT mice tumors (Figure 16). In contrast, myeloid cells including F4/80⁺ pan-macrophages and CD163⁺ M2-macrophage showed no difference between groups. Interestingly, tumor volume was negatively associated with the fractional area of CD8⁺ T

cells ($r^2=0.313$, $P<0.01$, Figure 17A), and positively associated with the fractional area of CD163⁺ macrophages ($r^2=0.309$, $P<0.01$, Figure 17B).

To gain further insights into the molecular characteristics of immune cells in the tumor microenvironments, mRNA expressions of immune cell-related genes were analyzed using whole tumor lysates. Consistently, the levels of *Cd4* and *Cd8* were significantly upregulated in the Col6a3-KO mice tumors compared to the WT mice tumors, indicating an increase in T cell populations. However, the expression of the pan T cell marker *Cd3* did not show a significant difference between the two groups (Figure 18). Additionally, the expression of *Cd69*, an early marker for T lymphocyte activation, and *Cd161*, a marker of NK cell function, was notably higher in the Col6a3-KO mice tumors compared to the WT mice tumors (Figure 18).

Furthermore, the expression of M1 macrophage markers, *Cd80* and *Cxcl10*, was significantly increased in the Col6a3-KO mice tumors compared to the WT mice tumors, suggesting an enhanced M1 polarization of macrophages. On the other hand, the expression of the immune suppressive M2 macrophage marker, *Arg1*, was reduced in the Col6a3-KO mice tumors compared to the WT mice tumors. The pan macrophage marker *F4/80*, however, did not show a significant difference between the two groups (Figure 18). Taken together, these findings indicate that the absence of ETP upregulates host-defensive immune responses in the tumor microenvironment. This results in a quantitative increase in cytotoxic T cells and a qualitative phenotypic change from M2 to M1 macrophages, indicating a shift towards

an anti-tumor immune response.

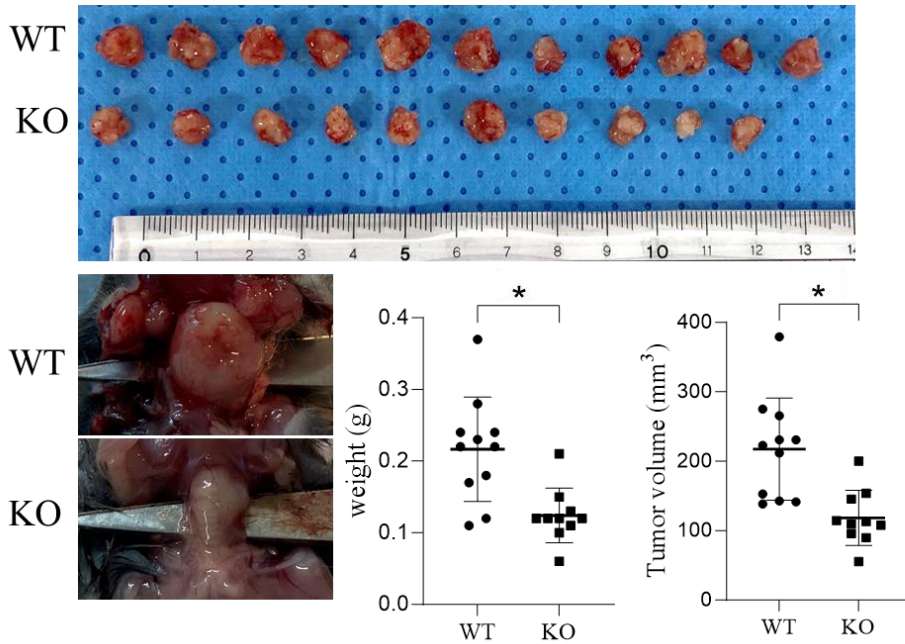


Figure 15. Reduced thyroid tumor growth in Col6a3-KO mice.

TBP3743-adapted cells ($10^5/10 \mu\text{L}$ PBS) were injected into the WT or Col6a3-KO murine thyroid via orthotopic injection. Tumors were harvested 2 weeks after injection. Representative images of tumors and quantification of tumor weight and volume are depicted. Data are presented as mean \pm SD.

* $p < 0.05$.

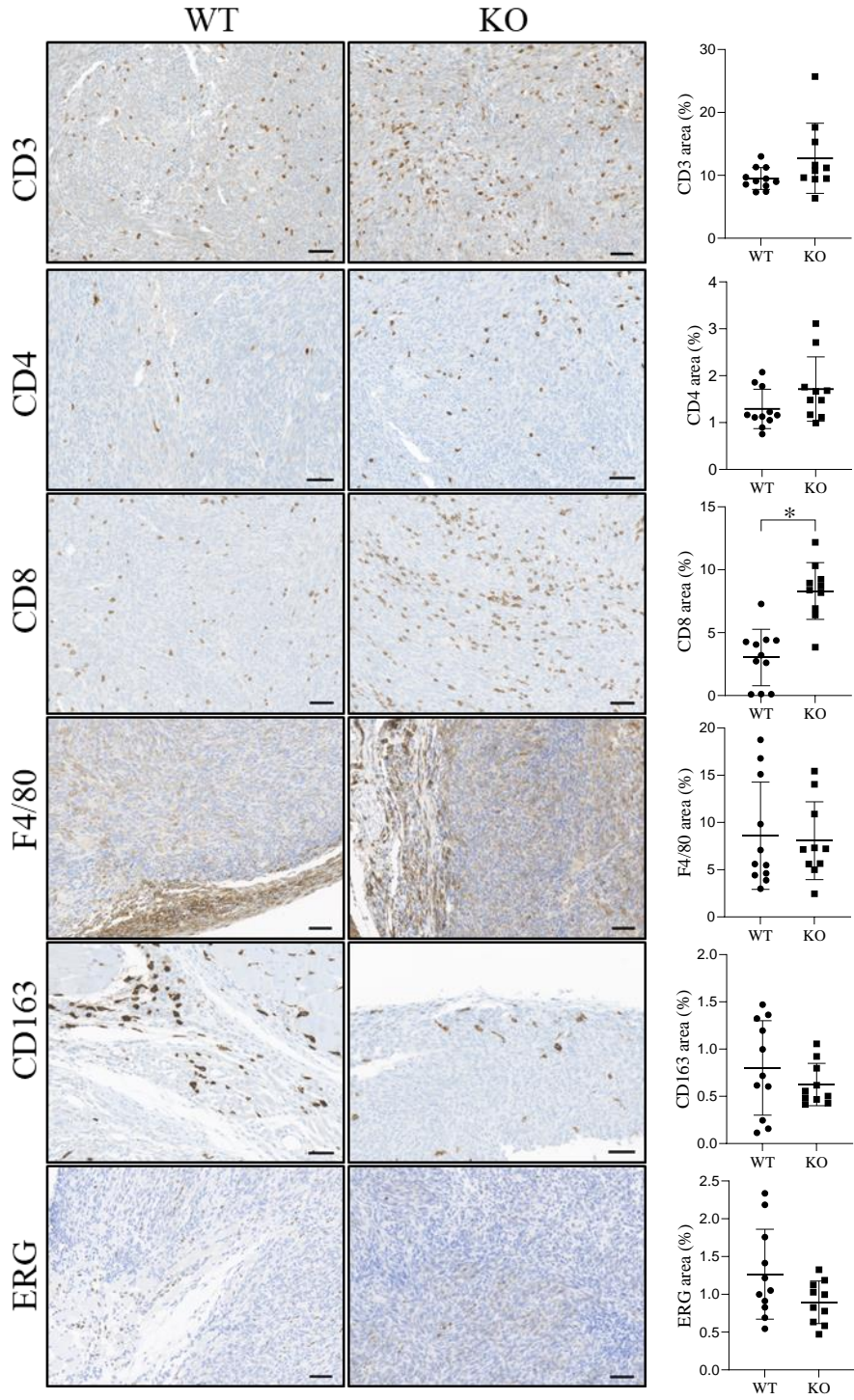


Figure 16. Expression of various cell types in mouse thyroid cancer.

TBP3743-adapted cells ($10^5/10 \mu\text{L}$ PBS) were injected into the WT or Col6a3-KO murine thyroid via orthotopic injection. Tumors were harvested 2 weeks after injection. Representative images of IHC for pan T cell (CD3), helper T cell (CD4), cytotoxic T cell (CD8), pan macrophage (F4/80), M2-macrophage (CD163), and endothelial cells (ERG) in each group of tumors. Scale bar: 50 μm . Data are presented as mean \pm SD. * $p < 0.05$. IHC, immunohistochemistry.

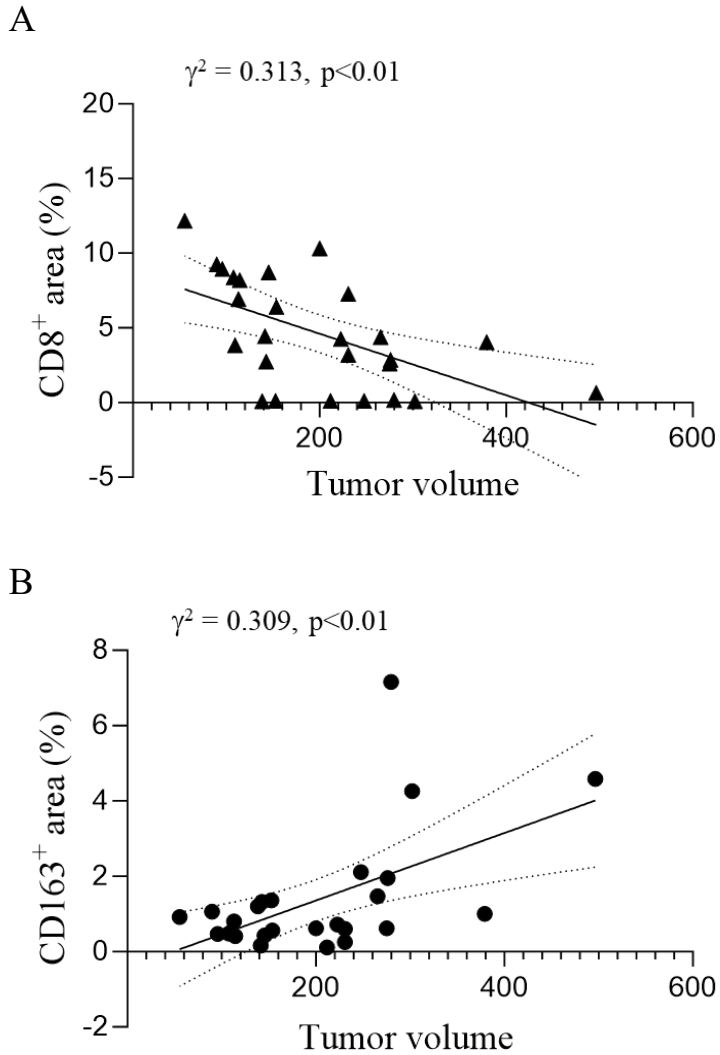


Figure 17. Correlation of tumor volume and immune cells.

TBP3743-adapted cells ($10^5/10 \mu\text{L}$ PBS) were injected into the WT or Col6a3-KO murine thyroid via orthotopic injection. Tumors were harvested 2 weeks after injection. A. CD8⁺ cells area are negatively correlated with tumor volume in mouse thyroid cancer tissues. B. CD163⁺ cells area are positively correlated with tumor volume in mouse thyroid cancer tissues.

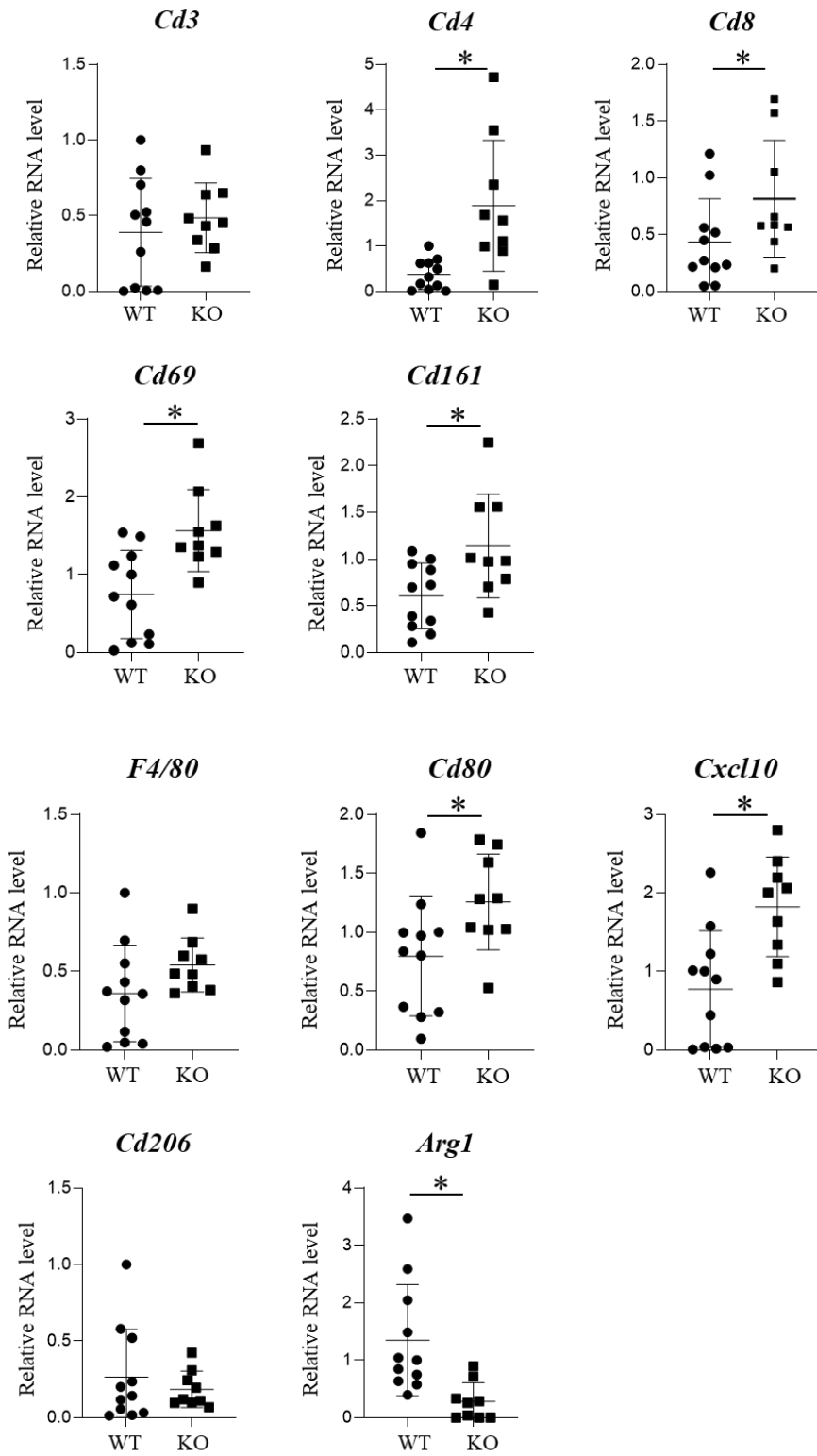


Figure 18. Expression of immune cell markers in mouse thyroid tumor.

TBP3743-adapted cells ($10^5/10 \mu\text{L}$ PBS) were injected into the WT or Col6a3-KO murine thyroid via orthotopic injection. Tumors were harvested 2 weeks after injection. A. T-lymphocytes (*Cd3* pan T; *Cd4* helper T; *Cd8* cytotoxic T; *Cd69* early activation T), NK cells (*Cd161*), and macrophages (*F4/80* pan macrophage; *Cd80* and *Cxcl10* M1-macrophage; *Cd206* and *Arg1* M2-macrophage) were analyzed by RT-qPCR analysis using whole tumor RNA. Data are presented as mean \pm SD. * $p < 0.05$.

3.8. ETP Interactions with the Tumor Microenvironment in Human Thyroid Cancer

To investigate the clinical relevance of ETP in human thyroid cancer, I analyzed RNA sequencing data from the SNUH thyroid cancer cohorts (95, 96). The dataset consisted of samples from normal thyroid tissue (n=86), papillary thyroid carcinoma (PTC) (n=125), and anaplastic thyroid carcinoma (ATC) (n=13). I found that the expression of *COL6A3*, the gene encoding ETP, was significantly higher in thyroid cancer (PTC and ATC) compared to normal tissues (Figure 19A). Moreover, among PTCs, *COL6A3* expression was significantly higher in BRAF-mutated PTCs compared to RAS-mutated PTCs (Figure 19B).

Next, I further analyzed the papillary thyroid carcinomas (PTCs) by dividing them into quartiles based on the expression levels of *COL6A3*. I performed gene set variation analysis (GSVA) using the Gene Ontology Biological Process (GOBP) gene set, and compared the results between the 1st quartile group (*COL6A3*-low/PTC) and the 4th quartile group (*COL6A3*-high/PTC). Interestingly, immune-related gene sets were found to be significantly upregulated in the *COL6A3*-high/PTC group compared to the *COL6A3*-low/PTC group (Figure 20).

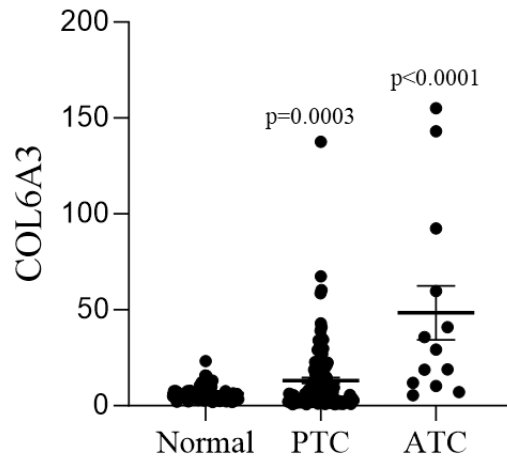
Furthermore, I examined the correlation between *COL6A3* expression and T cell- and macrophage-related genes in PTCs. I observed strong correlations between *COL6A3* expression and T cell-related genes, such as

FOXP3, *CD69*, *KLRB1*, and *CD4*, as well as macrophage-related genes, including *CD163* and *CD80* (Figure 21).

Similarly, I performed a similar analysis on anaplastic thyroid carcinomas (ATCs) by dividing them into quartiles based on the expression levels of *COL6A3*. I compared the results of GSVA using GOBP gene set between the 1st quartile group (COL6A3-low/ATC) and the 4th quartile group (COL6A3-high/ATC). Consistent with the findings in PTCs, I observed that immune-related gene sets were significantly upregulated in the COL6A3-high/ATC group compared to the COL6A3-low/ATC group (Figure 22).

Furthermore, I examined the correlation between *COL6A3* expression and T cell- and M2-macrophage-related genes in ATCs. I found strong correlations between *COL6A3* expression and T cell-related genes, such as *CD69* and *KLRB1*, as well as an M2-macrophage-specific gene, *CD81* (Figure 23). These results further support the potential role of *COL6A3* in modulating immune responses in thyroid cancers, particularly in relation to T cell and macrophage activities.

A



B

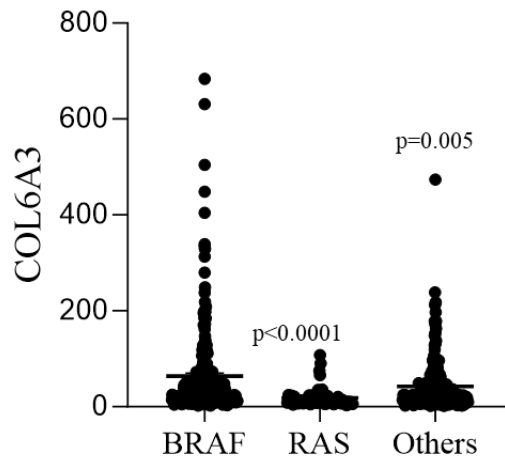


Figure 19. Expression of COL6A3 in human thyroid cancer.

RNA sequencing data from the SNUH thyroid cancer cohorts. A. Expression of *COL6A3*, the gene encoding ETP, in thyroid cancer (PTC and ATC) and normal tissues. B. Expression of *COL6A3* in BRAF-mutated PTCs, RAS-mutated PTCs and other-mutated PTCs.

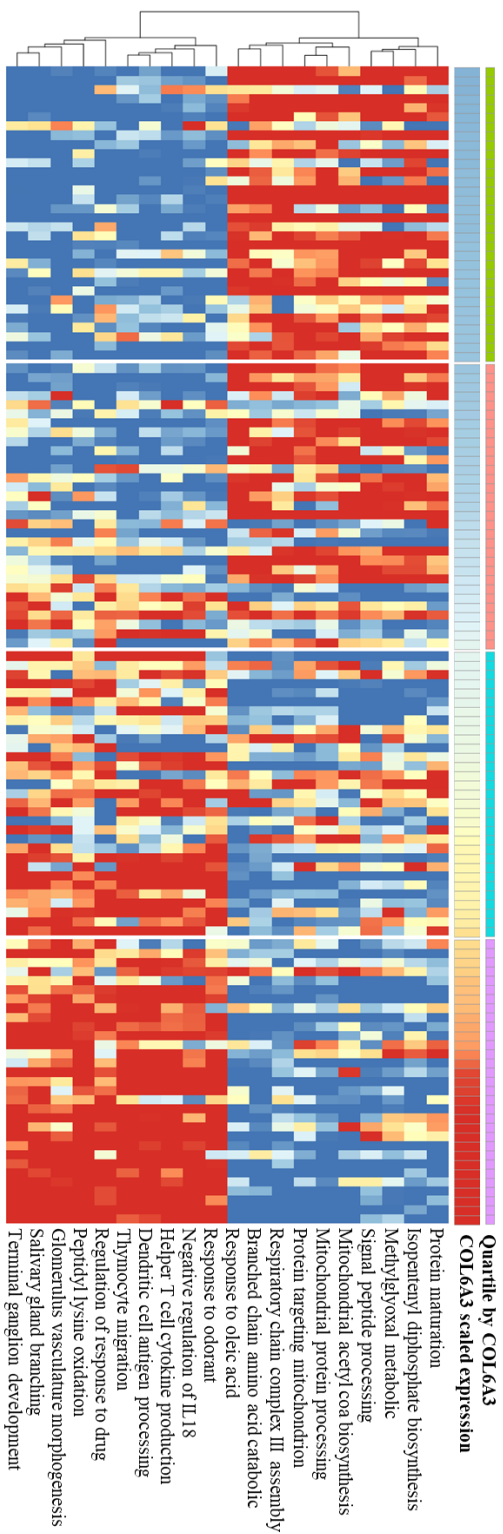


Figure 20. GO analysis of RNA-sequencing data in PTC.

Upregulation of immune-related gene sets in the COL6A3-high/PTC group compared to the COL6A3-low/PTC group.

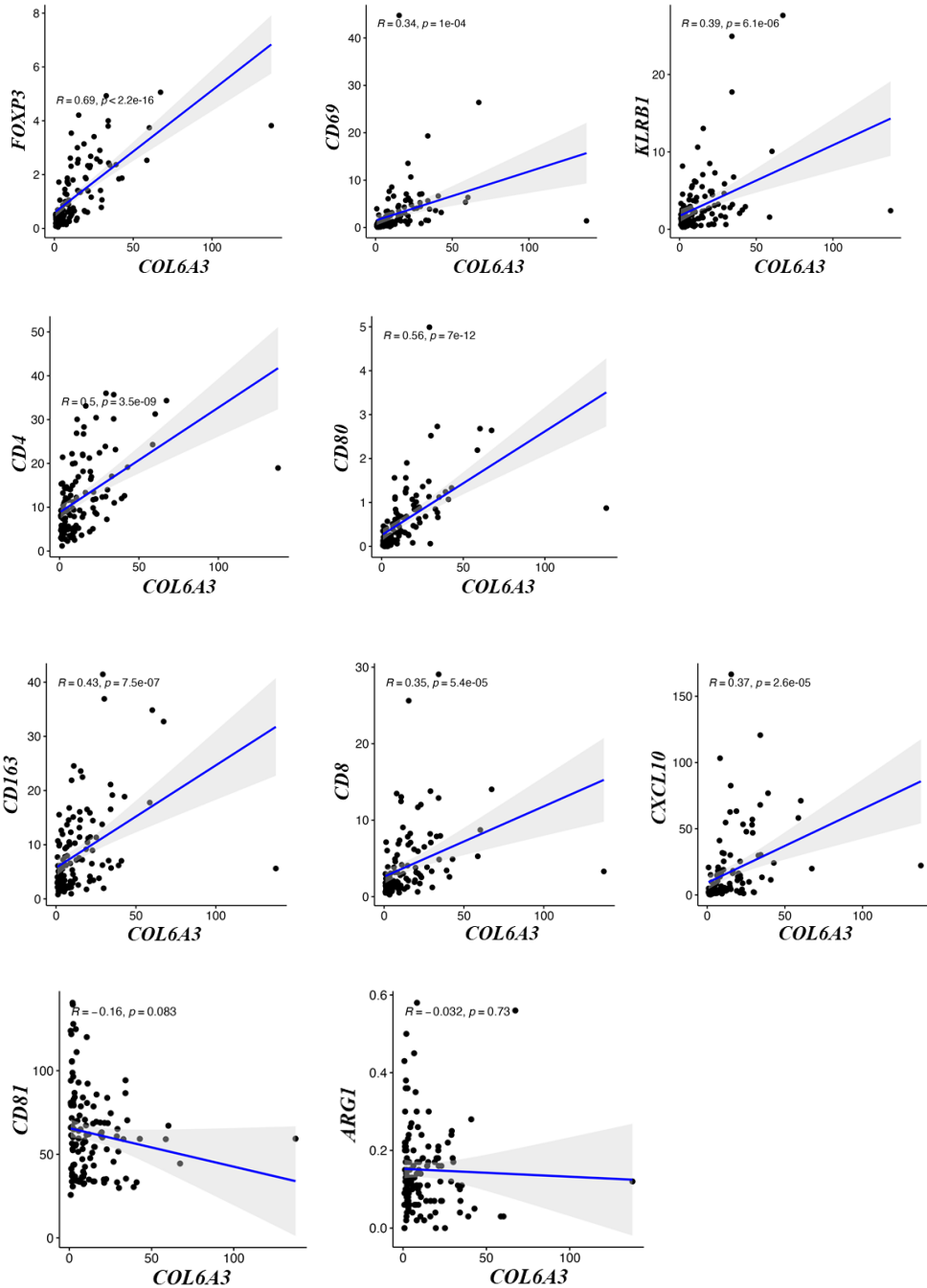


Figure 21. Correlation between COL6A3 and immune related genes in PTC.

Positively correlations between *COL6A3* expression and T cell-related genes.

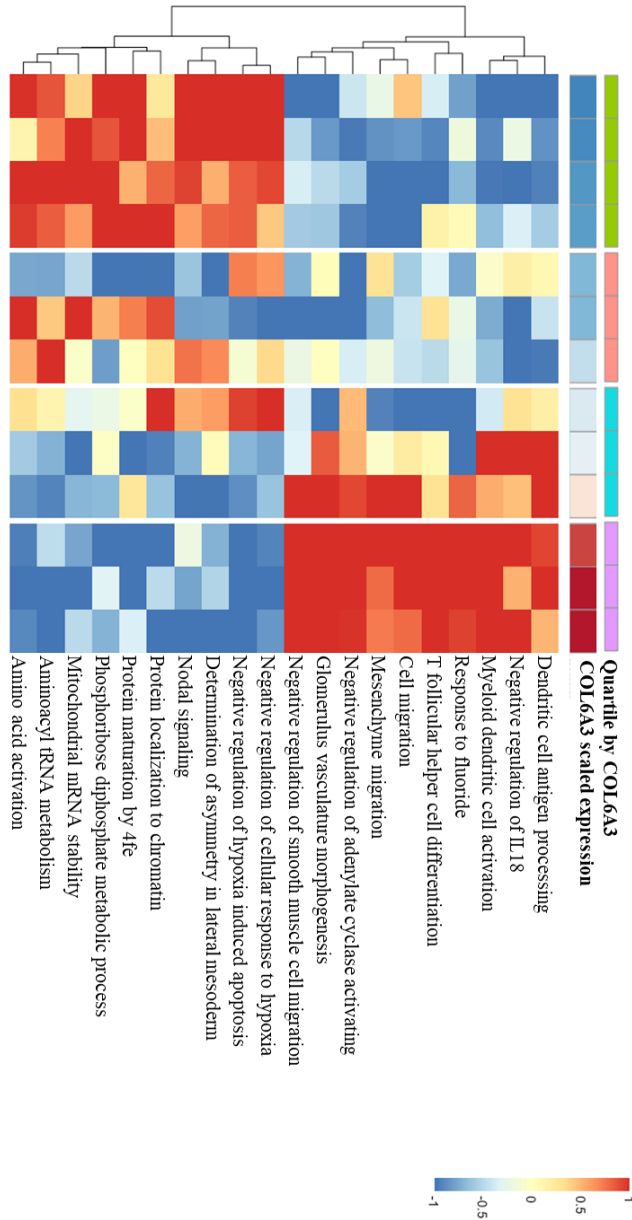


Figure 22. GO analysis of RNA-seq data in ATC.

Upregulation of immune-related gene sets in the COL6A3-high/ATC group compared to the COL6A3-low/ATC group.

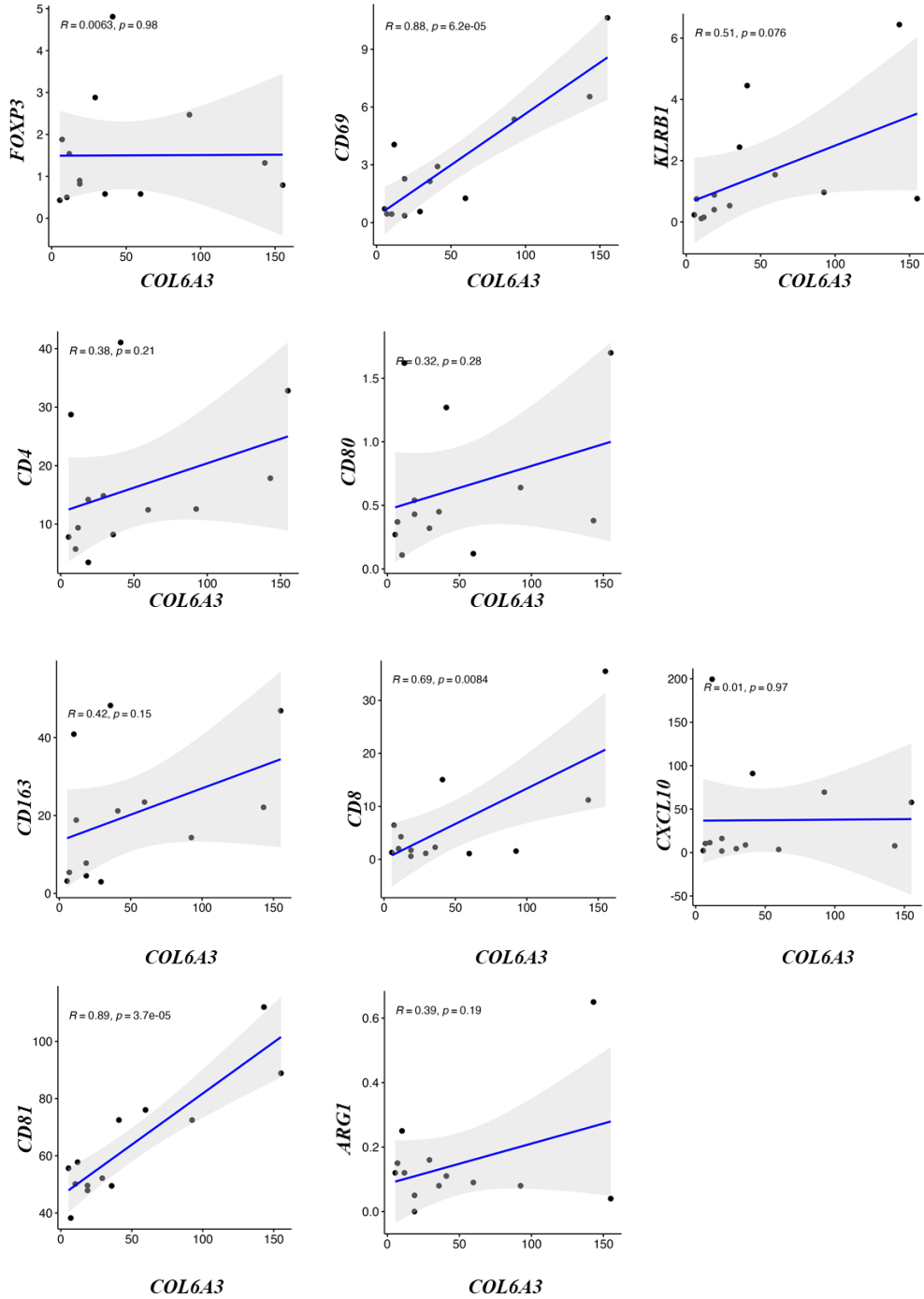


Figure 23. Correlation between COL6A3 and immune related genes in ATC.

Positively correlations between *COL6A3* expression and T cell-related genes.

3.9. MMP-9 and MMP-14 dependent production of ETP in macrophages

Previous studies have reported that the C5 domain of COL6A3 is cleaved by MMP-9 and MMP-14 in obesity models (97, 98). However, the mechanism underlying ETP production in the tumor microenvironment (TME) remains elusive. To address this, I analyzed RNA sequencing data from the SNUH thyroid cancer cohort and examined the correlation between MMPs and COL6A3. The heatmap analysis revealed that several MMPs, including MMP 9, 11, 13, and 16, exhibited positive correlations with COL6A3 expression (Figure 24A). Notably, MMP 9 and MMP 14 exhibited strong positive correlations with COL6A3 expression in both PTCs (Figure 24B) and ATCs (Figure 24C). Based on these findings, I hypothesize that MMP 9 and MMP 14 may play important roles in ETP production within the tumor-associated macrophage (TAM)-enriched TME of thyroid cancers.

PMA-stimulated THP-1 cells were treated with FRO-CM or BCPAP-CM for 24 hours, resulting in a significant induction of *MMP-9* and *MMP-14* expression (Figure 25). To investigate the functional role of CM-induced MMP-9 and MMP-14 in macrophages, co-cultures of THP-1 cells and FRO or BCPAP cells were treated with inhibitors targeting MMP-9 or MMP-14 (Figure 26A). Treatment with MMP-9 or MMP-14 inhibitors led to a significant reduction in secretory ETP protein compared to the control (Figure 26B).

To assess the effect of MMP-9 and MMP-14 inhibitor-treated CoCM, a cell migration assay was performed. The Transwell migration assay demonstrated that MMP-9 or MMP-14 inhibitor-treated CoCM decreased cell migration potential compared to CoCM alone, and treatment with ETP rescued this effect (Figure 26C). These findings collectively indicate that CM-induced MMP-9 and MMP-14 expression in THP-1 cells enhance the production of ETP through the cleavage of COL6A3.

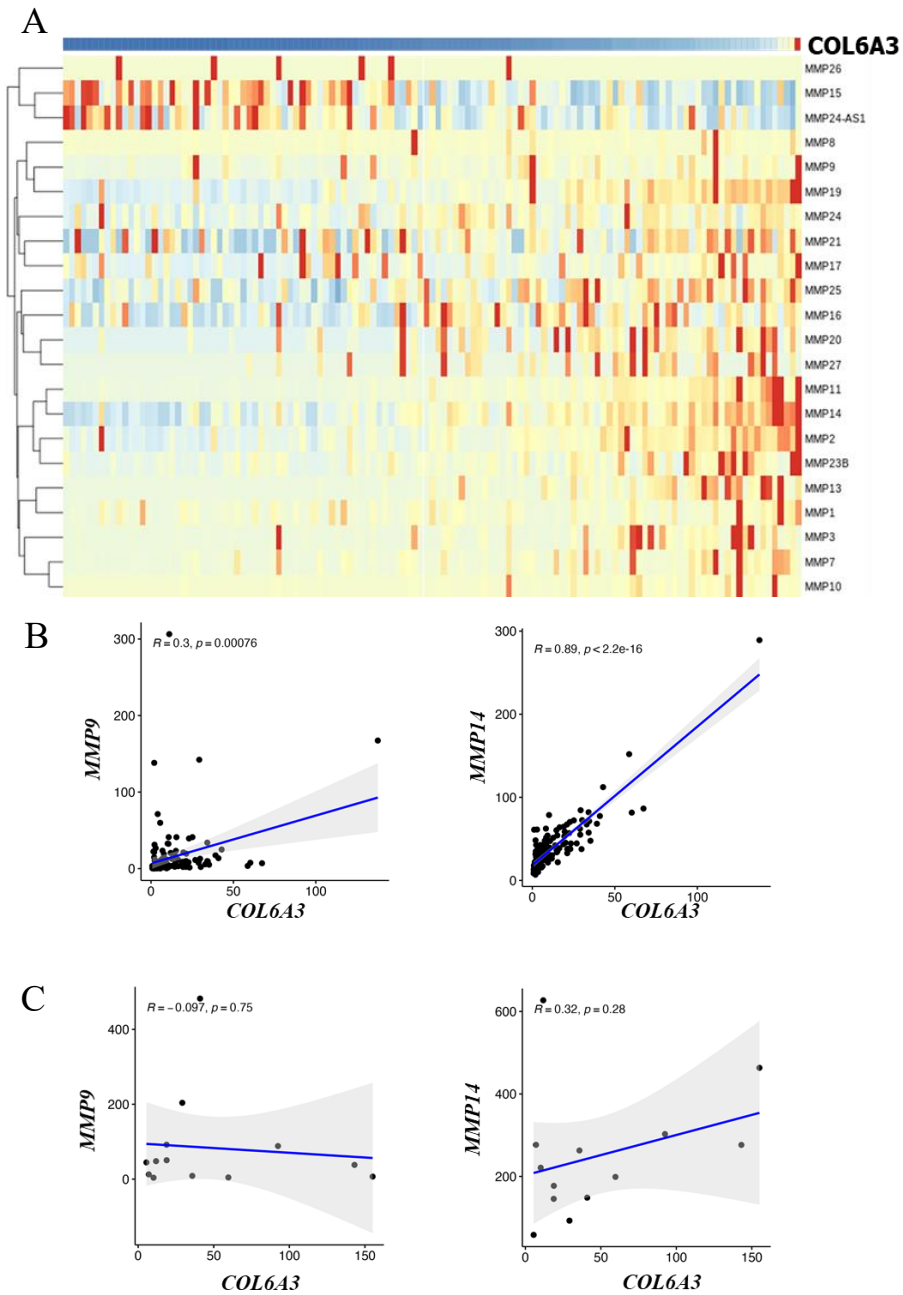


Figure 24. Analysis of MMPs associated with COL6A3 in thyroid cancers.

A. The heatmap represents the expression profile of MMPs associated with COL6A3 in thyroid cancers. B. Correlation between COL6A3 and MMPs in PTC. C. Correlation between COL6A3 and MMPs in ATC.

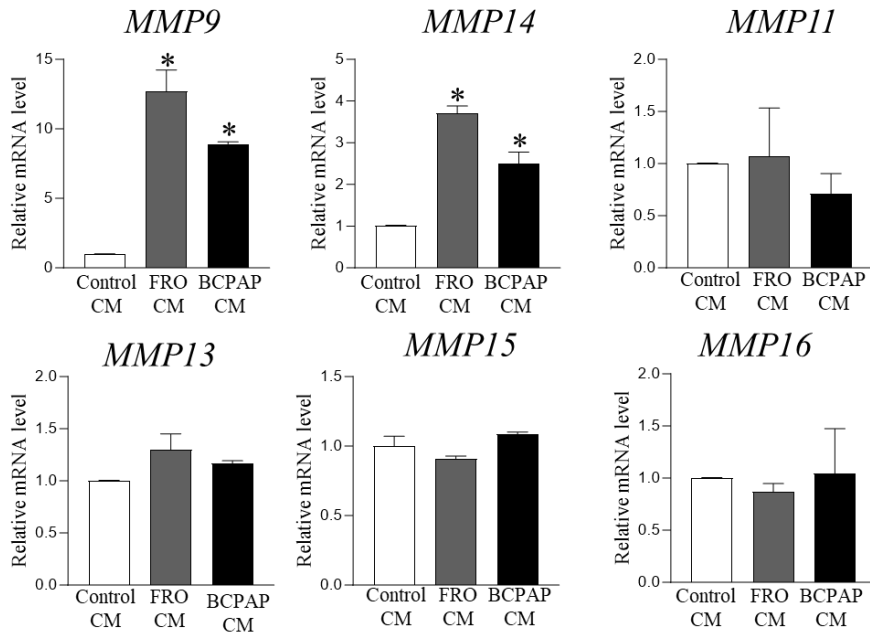


Figure 25. Expression of MMPs in CM-stimulated THP-1 cells.

PMA-stimulated THP-1 cells were treated with FRO- or BCPAP-CM to analyze the expression of MMPs by quantitative real-time PCR after 24 h. Data are presented as mean \pm SD. * $p < 0.05$. PMA, phorbol 12-myristate 13-acetate.

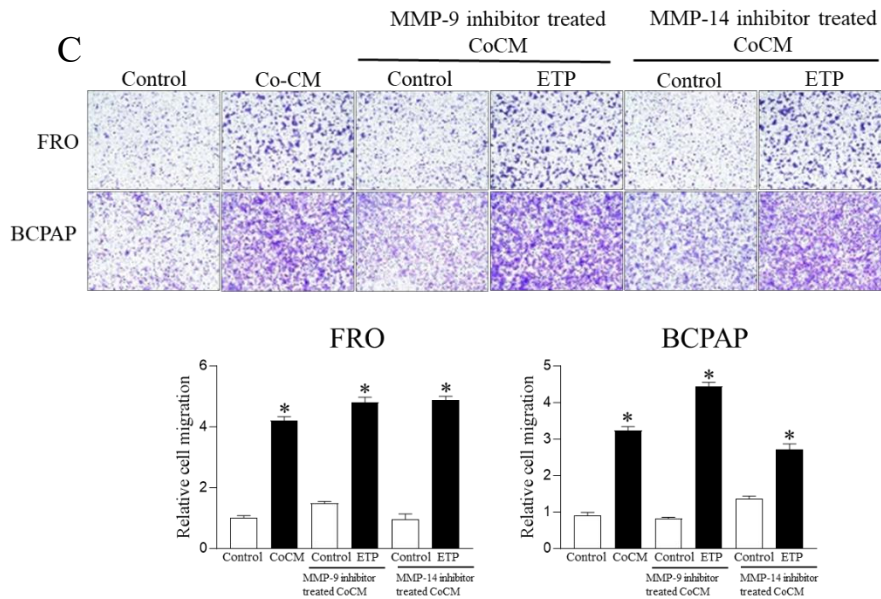
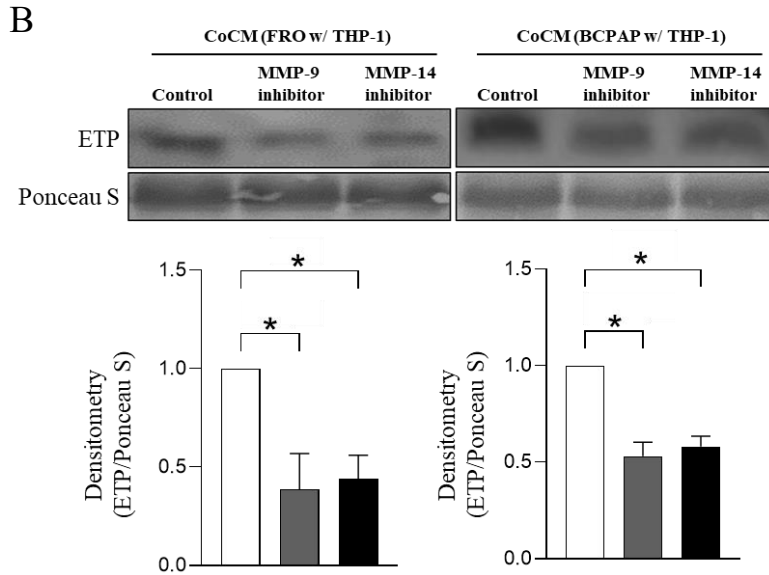
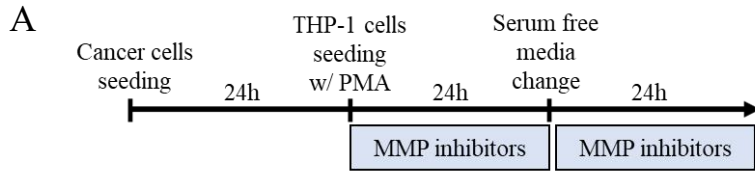


Figure 26. MMP-9 and MMP-14 cleaved COL6A3 to produce ETP in thyroid cancer cells CM-stimulated THP-1 cells.

A. Scheme of MMP-9 or MMP-14 inhibitor-treated CoCM. B. The secreted ETP in MMP-9 or MMP-14 inhibitor-treated CoCM was analyzed by western blot. C. FRO or BCPAP cells (10^5 cells/well) were inserted in the upper chamber and incubated with MMP-9 or MMP-14 inhibitor-treated CoCM and/or ETP in the bottom chamber for 12 h or 6 h, respectively. Data are presented as mean \pm SD. * $p < 0.05$. ETP, endotrophin; CoCM, co-culture conditioned medium.

4. Discussion

In this study, I demonstrated that macrophage-derived ETP plays a pro-tumorigenic role in the TME of thyroid cancer. IF staining showed the co-localization of CD163⁺ and ETP⁺ cells in mouse thyroid tumors. Moreover, ETP expression was increased by the co-culture of thyroid cancer cells and macrophages, leading to the induction of cancer cell migration by macrophage-derived ETP. Although cell proliferation did not affect the proliferation of thyroid cancer cells, tumor volume and weight were significantly greater in WT mice than in Col6a3-KO mice. The molecular analysis supported these results, demonstrating that expression of genes associated with oncogenic signaling pathways, such as JAK-STAT and TGF- β was enhanced in the FRO/WT-coCM-treated group compared with that in the FRO/KO-coCM-treated group in FRO cells. Furthermore, the mRNA levels of T lymphocytes, NK cell, and M1 macrophages were significantly upregulated in the Col6a3-KO mice tumors compared to the WT mice tumors. Hence, I suggest that ETP suppresses the immune response and promotes the progression to a more aggressive phenotype in the TME of patients with thyroid cancer.

Thyroid cancer can be triggered by genetic mutations, such as BRAF, RAS, and MAPK signaling pathways. The BRAF^{V600E} mutation is the most prevalent genetic mutation in PTC and ATC, while RAS mutations are frequently found in FTC and other PTC variants (99). It has been reported

that the presence of BRAF^{V600E} mutation can serve as a predictor for the aggressiveness of PTC and ATC (100-103). In an *in vivo* study demonstrated that high CXCL16 expression is linked to M2-macrophage infiltration in BRAF^{V600E} mutated PTC. This leads to tumor angiogenesis and a worse prognosis (78). In addition, CD163⁺ cells were increased in PTC with BRAF^{V600E} mutation than in PTC with BRAF^{WT} (104). Therefore, cell lines from human PTC and ATC with BRAF^{V600E} mutations, as well as mouse cell lines, were used in the study.

In the TME of thyroid cancer, TAM-derived CXCL8 increased PTC cells migration *in vitro*, and the administration of CXCL8 promoted metastasis to the lung *in vivo*. CXCL8 is an important mediator of the thyroid cancer microenvironment, promoting tumor growth and invasion (76). CXCL16, a chemokine protein, signaling in promoting tumor invasion of PTC through macrophage activation. CXCL16 expression was significantly higher in PTC tissues compared to adjacent normal tissues, and that it was associated with macrophage infiltration (77). Moreover, CXCL16 is correlated with the enhanced angiogenesis in thyroid cancer (78). TAM secreted Wnt1 and Wnt3a ligands, initiated Wnt signaling pathway and promoted the activation of β -catenin, which then induced proliferation and migration in thyroid cancer cells (105). TAM can also directly inhibit T cell activation via ARG1. ARG1 reduces the availability of L-arginine in the microenvironment, leading to decreased expression of the TCR-CD3 zeta chain on T cells, T cell proliferative arrest and impaired T cell function (50). Consequently, finding

the exact role of TAM in the TME is important for cancer treatment, including that of thyroid cancer. In this study, I presented TAM as one of the major cell types secreting ETP in the TME of thyroid cancer, ETP induced the thyroid cancer cells migration potential and immune suppressive microenvironment.

Park et al. reported that adipocyte-derived ETP is highly upregulated in adipose tissue, aggressive mammary tumor lesion. Additionally, ETP promotes metastatic growth via TGF- β -mediated epithelial-mesenchymal transition (EMT) of tumor cells (83). RNA-sequencing data revealed that genes related to cell migration were increased in ETP CM-treated thyroid cancer cells (Figure 15). Among chemotherapy, cisplatin is an anticancer drug used for various types of cancer, but its effectiveness decreases when resistance is developed. In a breast cancer mouse model administered with ETP neutralizing antibody, cisplatin resistance was decreased (84). Therefore, I suggest that targeting ETP in macrophage-enriched thyroid cancer might be a good strategy of chemotherapy. Moreover, ETP are strongly associated with poor prognosis in hepatocellular carcinoma (HCC) patients, and high expression of ETP in injured hepatocytes induced JNK-dependent hepatocyte apoptosis and activate nonparenchymal cells, leading to further activation of hepatic inflammation and fibrosis (106). The level of ETP was markedly upregulated in peripheral blood of breast cancer patients compared to cancer-free patients (85). Also, ETP has a potent stimulatory effect on tube formation in human endothelial cells (85). I observed that VEGFA, angiogenesis related genes, were increased in ETP CM-treated thyroid cancer cells (Figure 13).

Accordingly, these data suggest that ETP may support a pro-angiogenic role in TME of thyroid cancer.

ETP is secreted by adipocytes as an adipokine with potent tumor-promoting effects and has been studied as a marker of pro-tumorigenic cytokines in cancer (85). Despite the low proportion of adipocytes in thyroid cancer tissues, there was a significant increase in ETP staining in ATC tissues compared to PTC tissues. COL6A3 was upregulated in ATC positively correlated with TAM and ETP in IHC staining analysis. Interestingly, benign adenoma and autoimmune thyroiditis tissues did not show ETP expression upon IHC staining, whereas ETP expression was abundant in cancer tissues, especially in ATC. Notably, the density of TAM was increased in advanced thyroid cancers (56) and patients with ATC had higher density of CD163⁺ macrophages than the patients with PTC (86). Hence, I suggest that macrophage-derived ETP enhances the aggressive features of thyroid cancer by interacting with macrophages and cancer cells.

It has been reported that MMP-9 directly interacted with ETP and predominantly cleaved –L/M– sites at its C5 domain, generating 80-aa-long human ETP (97). Based on this evidence that the C5 domain of COL6A3 is cleaved by MMP-9, a collagenase, to generate ETP, and since MMP-9 is also abundantly expressed in macrophages, I investigated the role of MMP-9 in macrophages. As expected, blocking the activity of MMP-9 reduced the ETP production in macrophages. MMPs are proteases associated with ECM degradation that promote cancer progression (107, 108). CM from thyroid

cancer cells increased MMP-9 and MMP-14 levels in macrophages. These data indicate that stimulation of macrophages by thyroid cancer cells increases proteases, leading to remodeling of the ECM and resulting in a tumor-promoting TME.

Interestingly, the results of the IHC staining showed that CD8⁺ cells were increased in the Col6a3-KO mice tumors compared to the WT mice tumors (figure 16). Tumor growth was reduced in Col6a3-KO mice tumors compared to WT mice tumors, suggesting that a more active immune response inhibited tumor growth in Col6a3-KO mice. Furthermore, RT-qPCR analysis of tumor RNA revealed that expression of *Cd4*, *Cd8*, *Cd69*, *Cd161*, *Cd80*, and *Cxcl10* were increased in the Col6a3-KO mice tumors compared to the WT mice tumors. CD4 T cells, also known as helper T cells, play a crucial role in the tumor microenvironment. They are responsible for activating other immune cells, such as cytotoxic T cells and B cells, to help fight cancer (109). CD4 T cells also produce cytokines, which are signaling molecules that can help to regulate the immune response. In the TME, CD4 T cells can be found in different subsets, each with a distinct function. Th1 cells play a crucial role in directly eliminating tumor cells as they produce IFN- γ , which has cytotoxic effects on cancer cells. Additionally, IFN- γ plays a vital role in activating other immune cells like NK cells and cytotoxic T cells, enhancing their ability to recognize and eliminate tumor cells (110, 111). Th2 cells, on the other hand, produce IL-4, which promotes B cell responses. B cells are responsible for producing antibodies that can neutralize tumor cells. Through the production

of IL-4, Th2 cells support the generation of these antibodies, enhancing the immune response against tumors (112). Th17 cells produce IL-17, which aids in recruiting other immune cells to the tumor site. This recruitment of immune cells creates a more favorable environment for eliminating tumor cells. The additional immune cells recruited by IL-17 can collaborate to eliminate tumor cells or promote an anti-tumor immune response (113). CD8 T cells, as cytotoxic T cells, are able to directly kill tumor cells by recognizing and binding to specific peptides that are presented on the surface of the tumor cells by human leukocyte antigen class I (HLA-I) molecules (114). CD8 T cells are also able to produce cytokines such as perforin and granzymes, which are proteins that can cause the tumor cells to be eliminated. Perforin creates pores in the tumor cell membrane, allowing the entry of granzymes, which then initiate apoptosis, a process of programmed cell death (115). Additionally, cytokines that CD8 T cells secretes include IFN- γ , tumor necrosis factor-alpha (TNF- α), and IL-2 recruit other immune cells to the tumor site and help to suppress tumor growth (116-118). CD69 is a cell-surface protein that is expressed on activated T cells. CD69 is upregulated on T cells upon activation, and its expression can be induced by various stimuli, including T cell receptor (TCR) engagement and pro-inflammatory cytokines (119). The expression of CD69 is also regulated by transcription factors, such as NF- κ B and AP-1 (120, 121). CD69⁺ cells can help to promote the differentiation and activation of tumor-specific CD8⁺ T cells, to enhance the cytotoxicity of these cells, and to prevent the exhaustion of tumor-infiltrating

T cells. The exhaustion of tumor-infiltrating T cells is a major obstacle to effective cancer immunotherapy. This is because exhausted T cells are less able to proliferate and secrete cytokines, and they are more susceptible to apoptosis. CD69 has been shown to inhibit the exhaustion of tumor-infiltrating T cells by promoting their proliferation and survival (122). In addition to its effects on T cells, CD69 has also been shown to have effects on NK cells. NK cells are important effector cells of the innate immune system, and they play a role in the elimination of tumor cells. CD69 can help to enhance the cytotoxicity of NK cells (123, 124). CD161, also known as NKR-P1A or KLRB1, is a type II C-type lectin receptor expressed on the surface of NK cells, as well as certain subsets of T cells and innate lymphoid cells (125). NK cells are a type of cytotoxic lymphocyte that play a critical role in the immune system's defense against cancer. The anti-tumor effect of CD161⁺ NK cells is primarily attributed to their ability to recognize and eliminate tumor cells (126). CD161 is a receptor that binds to a molecule called lectin-like transcript 1 (LLT1), which is expressed on various types of tumor cells (127). The engagement of CD161 with LLT1 triggers a signaling cascade within the NK cell, inducing the activation of cytotoxic mechanisms. CD161⁺ NK cells release cytotoxic granules containing perforin and granzymes, which can directly induce cell death in tumor cells (128). Furthermore, CD161⁺ NK cells exhibit enhanced antibody-dependent cellular cytotoxicity (ADCC). ADCC occurs when NK cells recognize cancer cells opsonized with antibodies, such as monoclonal antibodies used in

immunotherapy (129). CD161 NK cells can bind to the Fc portion of these antibodies through their CD16 receptor, leading to the destruction of antibody-coated tumor cells. Hence, these data indicate an increase in the T cell and NK cell-mediated immune response, as well as an increase in M1 macrophages, which have anti-tumor activity. The increased infiltration of T cells, NK cells and M1 macrophages in the Col6a3-KO mice tumors strongly suggests that the absence of ETP has triggered an anti-tumor response within the TME.

Nevertheless, the precise origins and roles of ETP in the TME of thyroid cancer remain incompletely elucidated. The mechanism of ETP production is not known in a tissue-specific or pathologic condition-specific manner. Although studies have been conducted on several cancers, hepatic fibrosis, and adipose tissue dysfunction, research is still needed to understand the expression and role of ETP in various inflammatory pathophysiologies, including autoimmune diseases. Additionally, there is insufficient information on whether the cellular uptake of ETP is by ligand-receptor-mediated or endocytosis in the TME. Also, the effect of ETP on various immune cells such as T lymphocytes in the TME has not been investigated.

In conclusion, macrophage-derived ETP contributes to the immune inhibition of cancer and supports the pro-metastatic potential of human thyroid cancer in the TME. Thus, ETP may be a good therapeutic target for macrophage-enriched thyroid cancers.

5. Reference

1. Binnewies M, Roberts EW, Kersten K, Chan V, Fearon DF, Merad M, et al. Understanding the tumor immune microenvironment (TIME) for effective therapy. *Nat Med.* 2018;24(5):541-50.
2. Baghba R, Roshangar L, Jahanban-Esfahlan R, Seidi K, Ebrahimi-Kalan A, Jaymand M, et al. Tumor microenvironment complexity and therapeutic implications at a glance. *Cell Commun Signal.* 2020;18(1).
3. Mbeunkui F, Johann DJ. Cancer and the tumor microenvironment: a review of an essential relationship. *Cancer Chemoth Pharm.* 2009;63(4):571-82.
4. Smith HA, Kang Y. The metastasis-promoting roles of tumor-associated immune cells. *J Mol Med (Berl).* 2013;91(4):411-29.
5. Mantovani A, Marchesi F, Malesci A, Laghi L, Allavena P. Tumour-associated macrophages as treatment targets in oncology. *Nat Rev Clin Oncol.* 2017;14(7):399-416.
6. Waldman AD, Fritz JM, Lenardo MJ. A guide to cancer immunotherapy: from T cell basic science to clinical practice. *Nature Reviews Immunology.* 2020;20(11):651-68.
7. Li CX, Jiang P, Wei SH, Xu XF, Wang JJ. Regulatory T cells in tumor microenvironment: new mechanisms, potential therapeutic strategies and future prospects. *Mol Cancer.* 2020;19(1).
8. Sahai E, Astsaturov I, Cukierman E, DeNardo DG, Egeblad M, Evans RM, et al. A framework for advancing our understanding of cancer-associated

fibroblasts. *Nat Rev Cancer*. 2020;20(3):174-86.

9. Vesely MD, Kershaw MH, Schreiber RD, Smyth MJ. Natural innate and adaptive immunity to cancer. *Annu Rev Immunol*. 2011;29:235-71.

10. Waldman AD, Fritz JM, Lenardo MJ. A guide to cancer immunotherapy: from T cell basic science to clinical practice. *Nat Rev Immunol*. 2020;20(11):651-68.

11. Gajewski TF, Woo SR, Zha YY, Spaapen R, Zheng Y, Corrales L, et al. Cancer immunotherapy strategies based on overcoming barriers within the tumor microenvironment. *Curr Opin Immunol*. 2013;25(2):268-76.

12. Lawrence MS, Stojanov P, Polak P, Kryukov GV, Cibulskis K, Sivachenko A, et al. Mutational heterogeneity in cancer and the search for new cancer-associated genes. *Nature*. 2013;499(7457):214-8.

13. Gajewski TF. Cancer immunotherapy. *Mol Oncol*. 2012;6(2):242-50.

14. Galluzzi L, Vacchelli E, Bravo-San Pedro JM, Buque A, Senovilla L, Baracco EE, et al. Classification of current anticancer immunotherapies. *Oncotarget*. 2014;5(24):12472-508.

15. Marincola FM, Wang E, Herlyn M, Seliger B, Ferrone S. Tumors as elusive targets of T-cell-based active immunotherapy. *Trends Immunol*. 2003;24(6):335-42.

16. Melero I, Gaudemack G, Gerritsen W, Huber C, Parmiani G, Scholl S, et al. Therapeutic vaccines for cancer: an overview of clinical trials. *Nat Rev Clin Oncol*. 2014;11(9):509-24.

17. Maher J, Davies ET. Targeting cytotoxic T lymphocytes for cancer

- immunotherapy. *Br J Cancer*. 2004;91(5):817-21.
18. June CH, O'Connor RS, Kawalekar OU, Ghassemi S, Milone MC. CAR T cell immunotherapy for human cancer. *Science*. 2018;359(6382):1361-5.
 19. Pardoll DM. The blockade of immune checkpoints in cancer immunotherapy. *Nat Rev Cancer*. 2012;12(4):252-64.
 20. Pennock GK, Chow LQM. The Evolving Role of Immune Checkpoint Inhibitors in Cancer Treatment. *Oncologist*. 2015;20(7):812-22.
 21. He X, Xu C. Immune checkpoint signaling and cancer immunotherapy. *Cell Res*. 2020;30(8):660-9.
 22. Khoja L, Butler MO, Kang SP, Ebbinghaus S, Joshua AM. Pembrolizumab. *J Immunother Cancer*. 2015;3:36.
 23. Brahmer JR, Hammers H, Lipson EJ. Nivolumab: targeting PD-1 to bolster antitumor immunity. *Future Oncol*. 2015;11(9):1307-26.
 24. Buchbinder EI, Desai A. CTLA-4 and PD-1 Pathways: Similarities, Differences, and Implications of Their Inhibition. *Am J Clin Oncol*. 2016;39(1):98-106.
 25. Alegre ML, Frauwirth KA, Thompson CB. T-cell regulation by CD28 and CTLA-4. *Nat Rev Immunol*. 2001;1(3):220-8.
 26. Leach DR, Krummel MF, Allison JP. Enhancement of antitumor immunity by CTLA-4 blockade. *Science*. 1996;271(5256):1734-6.
 27. Chambers CA, Kuhns MS, Egen JG, Allison JP. CTLA-4-mediated inhibition in regulation of T cell responses: mechanisms and manipulation in

- tumor immunotherapy. *Annu Rev Immunol.* 2001;19:565-94.
28. Bardhan K, Anagnostou T, Boussiotis VA. The PD1:PD-L1/2 Pathway from Discovery to Clinical Implementation. *Front Immunol.* 2016;7:550.
 29. Akinleye A, Rasool Z. Immune checkpoint inhibitors of PD-L1 as cancer therapeutics. *Journal of Hematology & Oncology.* 2019;12(1).
 30. Lake RA, Robinson BW. Immunotherapy and chemotherapy--a practical partnership. *Nat Rev Cancer.* 2005;5(5):397-405.
 31. Salas-Benito D, Perez-Gracia JL, Ponz-Sarvise M, Rodriguez-Ruiz ME, Martinez-Forero I, Castanon E, et al. Paradigms on Immunotherapy Combinations with Chemotherapy. *Cancer Discov.* 2021;11(6):1353-67.
 32. Liu YT, Sun ZJ. Turning cold tumors into hot tumors by improving T-cell infiltration. *Theranostics.* 2021;11(11):5365-86.
 33. Bonaventura P, Shekarian T, Alcazer V, Valladeau-Guilemond J, Valsesia-Wittmann S, Amigorena S, et al. Cold Tumors: A Therapeutic Challenge for Immunotherapy. *Front Immunol.* 2019;10:168.
 34. Johnson DB, Sullivan RJ, Menzies AM. Immune checkpoint inhibitors in challenging populations. *Cancer.* 2017;123(11):1904-11.
 35. Abdel-Wahab N, Shah M, Lopez-Olivo MA, Suarez-Almazor ME. Use of Immune Checkpoint Inhibitors in the Treatment of Patients With Cancer and Preexisting Autoimmune Disease: A Systematic Review. *Ann Intern Med.* 2018;168(2):121-30.
 36. Pan YY, Yu YD, Wang XJ, Zhang T. Tumor-Associated Macrophages

- in Tumor Immunity (vol 11, 583084, 2020). *Front Immunol.* 2021;12.
37. Murray PJ. Macrophage Polarization. *Annu Rev Physiol.* 2017;79:541-66.
38. Orecchioni M, Ghosheh Y, Pramod AB, Ley K. Macrophage Polarization: Different Gene Signatures in M1(LPS+) vs. Classically and M2(LPS-) vs. Alternatively Activated Macrophages (vol 10, 1084, 2019). *Front Immunol.* 2020;11.
39. Schroder K, Hertzog PJ, Ravasi T, Hume DA. Interferon-gamma: an overview of signals, mechanisms and functions. *J Leukoc Biol.* 2004;75(2):163-89.
40. Shapouri-Moghaddam A, Mohammadian S, Vazini H, Taghadosi M, Esmaeili SA, Mardani F, et al. Macrophage plasticity, polarization, and function in health and disease. *J Cell Physiol.* 2018;233(9):6425-40.
41. Sica A, Schioppa T, Mantovani A, Allavena P. Tumour-associated macrophages are a distinct M2 polarised population promoting tumour progression: potential targets of anti-cancer therapy. *Eur J Cancer.* 2006;42(6):717-27.
42. Solinas G, Germano G, Mantovani A, Allavena P. Tumor-associated macrophages (TAM) as major players of the cancer-related inflammation. *J Leukocyte Biol.* 2009;86(5):1065-73.
43. Sato T, Terai M, Tamura Y, Alexeev V, Mastrangelo MJ, Selvan SR. Interleukin 10 in the tumor microenvironment: a target for anticancer immunotherapy. *Immunol Res.* 2011;51(2-3):170-82.

44. Flavell RA, Sanjabi S, Wrzesinski SH, Licona-Limon P. The polarization of immune cells in the tumour environment by TGFbeta. *Nat Rev Immunol.* 2010;10(8):554-67.
45. Lim SY, Yuzhalin AE, Gordon-Weeks AN, Muschel RJ. Targeting the CCL2-CCR2 signaling axis in cancer metastasis. *Oncotarget.* 2016;7(19):28697-710.
46. Mantovani A, Biswas SK, Galdiero MR, Sica A, Locati M. Macrophage plasticity and polarization in tissue repair and remodelling. *J Pathol.* 2013;229(2):176-85.
47. Schutysse E, Richmond A, Van Damme J. Involvement of CC chemokine ligand 18 (CCL18) in normal and pathological processes. *J Leukoc Biol.* 2005;78(1):14-26.
48. Chanmee T, Ontong P, Konno K, Itano N. Tumor-Associated Macrophages as Major Players in the Tumor Microenvironment. *Cancers.* 2014;6(3):1670-90.
49. Mantovani A, Sica A. Macrophages, innate immunity and cancer: balance, tolerance, and diversity. *Curr Opin Immunol.* 2010;22(2):231-7.
50. Arlauckas SP, Garren SB, Garris CS, Kohler RH, Oh J, Pittet MJ, et al. Arg1 expression defines immunosuppressive subsets of tumor-associated macrophages. *Theranostics.* 2018;8(21):5842-54.
51. Roszer T. Understanding the Mysterious M2 Macrophage through Activation Markers and Effector Mechanisms. *Mediat Inflamm.* 2015;2015.
52. Qiu SQ, Waaijer SJH, Zwager MC, de Vries EGE, van der Vegt B,

Schroder CP. Tumor-associated macrophages in breast cancer: Innocent bystander or important player? *Cancer Treat Rev.* 2018;70:178-89.

53. Sumitomo R, Hirai T, Fujita M, Murakami H, Otake Y, Huang CL. M2 tumor-associated macrophages promote tumor progression in non-small-cell lung cancer. *Exp Ther Med.* 2019;18(6):4490-8.

54. Arvanitakis K, Koletsa T, Mitroulis I, Germanidis G. Tumor-Associated Macrophages in Hepatocellular Carcinoma Pathogenesis, Prognosis and Therapy. *Cancers (Basel).* 2022;14(1).

55. Leblond MM, Zdimerova H, Desponds E, Verdeil G. Tumor-Associated Macrophages in Bladder Cancer: Biological Role, Impact on Therapeutic Response and Perspectives for Immunotherapy. *Cancers (Basel).* 2021;13(18).

56. Ryder M, Ghossein RA, Ricarte JCM, Knauf JA, Fagin JA. Increased density of tumor-associated macrophages is associated with decreased survival in advanced thyroid cancer. *Endocr-Relat Cancer.* 2008;15(4):1069-74.

57. Katz JB, Muller AJ, Prendergast GC. Indoleamine 2,3-dioxygenase in T-cell tolerance and tumoral immune escape. *Immunol Rev.* 2008;222:206-21.

58. Czystowska-Kuzmich M, Sosnowska A, Nowis D, Ramji K, Szajnik M, Chlebowska-Tuz J, et al. Small extracellular vesicles containing arginase-1 suppress T-cell responses and promote tumor growth in ovarian carcinoma. *Nature Communications.* 2019;10.

59. Ngambenjawong C, Gustafson HH, Pun SH. Progress in tumor-associated macrophage (TAM)-targeted therapeutics. *Adv Drug Deliv Rev.* 2017;114:206-21.
60. Kohli K, Pillarisetty VG, Kim TS. Key chemokines direct migration of immune cells in solid tumors. *Cancer Gene Ther.* 2022;29(1):10-21.
61. Cannarile MA, Weisser M, Jacob W, Jegg AM, Ries CH, Ruttinger D. Colony-stimulating factor 1 receptor (CSF1R) inhibitors in cancer therapy. *J Immunother Cancer.* 2017;5(1):53.
62. Acharya N, Sabatos-Peyton C, Anderson AC. Tim-3 finds its place in the cancer immunotherapy landscape. *J Immunother Cancer.* 2020;8(1).
63. Yang J, Yan J, Liu B. Targeting VEGF/VEGFR to Modulate Antitumor Immunity. *Front Immunol.* 2018;9:978.
64. Duan ZJ, Luo YP. Targeting macrophages in cancer immunotherapy. *Signal Transduct Tar.* 2021;6(1).
65. Ruffell B, Coussens LM. Macrophages and therapeutic resistance in cancer. *Cancer Cell.* 2015;27(4):462-72.
66. Logtenberg MEW, Scheeren FA, Schumacher TN. The CD47-SIRPalpha Immune Checkpoint. *Immunity.* 2020;52(5):742-52.
67. Weiskopf K. Cancer immunotherapy targeting the CD47/SIRPalpha axis. *Eur J Cancer.* 2017;76:100-9.
68. Chao MP, Weissman IL, Majeti R. The CD47-SIRPalpha pathway in cancer immune evasion and potential therapeutic implications. *Curr Opin Immunol.* 2012;24(2):225-32.

69. Lu Q, Chen X, Wang S, Lu Y, Yang C, Jiang G. Potential New Cancer Immunotherapy: Anti-CD47-SIRPalpha Antibodies. *Onco Targets Ther.* 2020;13:9323-31.
70. Keutgen XM, Sadowski SM, Kebebew E. Management of anaplastic thyroid cancer. *Gland Surg.* 2015;4(1):44-51.
71. Caronia LM, Phay JE, Shah MH. Role of BRAF in thyroid oncogenesis. *Clin Cancer Res.* 2011;17(24):7511-7.
72. Begum S, Rosenbaum E, Henrique R, Cohen Y, Sidransky D, Westra WH. BRAF mutations in anaplastic thyroid carcinoma: implications for tumor origin, diagnosis and treatment. *Modern Pathol.* 2004;17(11):1359-63.
73. Xing M. BRAF mutation in thyroid cancer. *Endocr Relat Cancer.* 2005;12(2):245-62.
74. Kim DI, Kim E, Kim YA, Cho SW, Lim JA, Park YJ. Macrophage Densities Correlated with CXC Chemokine Receptor 4 Expression and Related with Poor Survival in Anaplastic Thyroid Cancer. *Endocrinol Metab (Seoul).* 2016;31(3):469-75.
75. Kim S, Cho SW, Min HS, Kim KM, Yeom GJ, Kim EY, et al. The expression of tumor-associated macrophages in papillary thyroid carcinoma. *Endocrinol Metab (Seoul).* 2013;28(3):192-8.
76. Fang W, Ye L, Shen L, Cai J, Huang F, Wei Q, et al. Tumor-associated macrophages promote the metastatic potential of thyroid papillary cancer by releasing CXCL8. *Carcinogenesis.* 2014;35(8):1780-7.
77. Cho SW, Kim YA, Sun HJ, Kim YA, Oh BC, Yi KH, et al. CXCL16

signaling mediated macrophage effects on tumor invasion of papillary thyroid carcinoma. *Endocr Relat Cancer*. 2016;23(2):113-24.

78. Kim MJ, Sun HJ, Song YS, Yoo SK, Kim YA, Seo JS, et al. CXCL16 positively correlated with M2-macrophage infiltration, enhanced angiogenesis, and poor prognosis in thyroid cancer. *Sci Rep-Uk*. 2019;9.

79. Henke E, Nandigama R, Ergun S. Extracellular Matrix in the Tumor Microenvironment and Its Impact on Cancer Therapy. *Front Mol Biosci*. 2019;6:160.

80. Brassart-Pasco S, Brezillon S, Brassart B, Ramont L, Oudart JB, Monboisse JC. Tumor Microenvironment: Extracellular Matrix Alterations Influence Tumor Progression. *Front Oncol*. 2020;10.

81. Winkler J, Abisoye-Ogunniyan A, Metcalf KJ, Werb Z. Concepts of extracellular matrix remodelling in tumour progression and metastasis. *Nat Commun*. 2020;11(1):5120.

82. Cescon M, Gattazzo F, Chen PW, Bonaldo P. Collagen VI at a glance. *J Cell Sci*. 2015;128(19):3525-31.

83. Park J, Scherer PE. Adipocyte-derived endotrophin promotes malignant tumor progression. *J Clin Invest*. 2012;122(11):4243-56.

84. Park J, Morley TS, Scherer PE. Inhibition of endotrophin, a cleavage product of collagen VI, confers cisplatin sensitivity to tumours. *Embo Mol Med*. 2013;5(6):935-48.

85. Bu DW, Crewe C, Kusminski CM, Gordillo R, Ghaben AL, Kim M, et al. Human endotrophin as a driver of malignant tumor growth. *Jci Insight*.

2019;4(9).

86. Jung KY, Cho SW, Kim YA, Kim D, Oh BC, Park DJ, et al. Cancers with Higher Density of Tumor-Associated Macrophages Were Associated with Poor Survival Rates. *J Pathol Transl Med.* 2015;49(4):318-24.

87. Fluge O, Bruland O, Akslen LA, Lillehaug JR, Varhaug JE. Gene expression in poorly differentiated papillary thyroid carcinomas. *Thyroid.* 2006;16(2):161-75.

88. Montero-Conde C, Martin-Campos JM, Lerma E, Gimenez G, Martinez-Guitarte JL, Combalia N, et al. Molecular profiling related to poor prognosis in thyroid carcinoma. Combining gene expression data and biological information. *Oncogene.* 2008;27(11):1554-61.

89. Daigneault M, Preston JA, Marriott HM, Whyte MK, Dockrell DH. The identification of markers of macrophage differentiation in PMA-stimulated THP-1 cells and monocyte-derived macrophages. *PLoS One.* 2010;5(1):e8668.

90. Vanden Borre P, McFadden DG, Gunda V, Sadow PM, Varmeh S, Bernasconi M, et al. The next generation of orthotopic thyroid cancer models: immunocompetent orthotopic mouse models of BRAF V600E-positive papillary and anaplastic thyroid carcinoma. *Thyroid.* 2014;24(4):705-14.

91. Lemoine NR, Mayall ES, Jones T, Sheer D, Mcdermid S, Kendall-taylor P, et al. Characterization of Human Thyroid Epithelial-Cells Immortalized In vitro by Simian-Virus 40-DNA Transfection. *Brit J Cancer.* 1989;60(6):897-903.

92. Xu J, Lamouille S, Derynck R. TGF-beta-induced epithelial to mesenchymal transition. *Cell Research*. 2009;19(2):156-72.
93. Teng Y, Ross JL, Cowell JK. The involvement of JAK-STAT3 in cell motility, invasion, and metastasis. *JAKSTAT*. 2014;3(1):e28086.
94. Xie J, Liu Y, Du X, Wu Y. TGF-beta1 promotes the invasion and migration of papillary thyroid carcinoma cells by inhibiting the expression of lncRNA-NEF. *Oncol Lett*. 2019;17(3):3125-32.
95. Yoo SK, Lee S, Kim SJ, Jee HG, Kim BA, Cho H, et al. Comprehensive Analysis of the Transcriptional and Mutational Landscape of Follicular and Papillary Thyroid Cancers. *PLoS Genet*. 2016;12(8):e1006239.
96. Yoo SK, Song YS, Lee EK, Hwang J, Kim HH, Jung G, et al. Integrative analysis of genomic and transcriptomic characteristics associated with progression of aggressive thyroid cancer. *Nat Commun*. 2019;10(1):2764.
97. Jo W, Kim M, Oh J, Kim CS, Park C, Yoon S, et al. MicroRNA-29 Ameliorates Fibro-Inflammation and Insulin Resistance in HIF1 alpha-Deficient Obese Adipose Tissue by Inhibiting Endotrophin Generation. *Diabetes*. 2022;71(8):1746-62.
98. Li X, Zhao Y, Chen C, Yang L, Lee HH, Wang Z, et al. Critical Role of Matrix Metalloproteinase 14 in Adipose Tissue Remodeling during Obesity. *Mol Cell Biol*. 2020;40(8).
99. Liu Q, Sun W, Zhang H. Roles and new Insights of Macrophages in the Tumor Microenvironment of Thyroid Cancer. *Front Pharmacol*.

2022;13:875384.

100. Xing MZ, Alzahrani AS, Carson KA, Viola D, Elisei R, Bendlova B, et al. Association Between BRAF V600E Mutation and Mortality in Patients With Papillary Thyroid Cancer. *Jama-J Am Med Assoc.* 2013;309(14):1493-501.

101. Li C, Lee KC, Schneider EB, Zeiger MA. BRAF V600E mutation and Its Association with Clinicopathological Features of Papillary Thyroid Cancer: A Meta-Analysis. *J Clin Endocr Metab.* 2012;97(12):4559-70.

102. Rao SN, Zafereo M, Dadu R, Busaidy NL, Hess K, Cote GJ, et al. Patterns of Treatment Failure in Anaplastic Thyroid Carcinoma. *Thyroid.* 2017;27(5):672-81.

103. Choi S, Shugard E, Khanafshar E, Quivey JM, Garsa AA, Yom SS. Association Between BRAF V600E Mutation and Decreased Survival in Patients Locoregionally Irradiated for Anaplastic Thyroid Carcinoma. *Int J Radiat Oncol.* 2016;96(2):E356-E.

104. Angell TE, Lechner MG, Jang JK, Correa AJ, LoPresti JS, Epstein AL. BRAF(V600E) in Papillary Thyroid Carcinoma Is Associated with Increased Programmed Death Ligand 1 Expression and Suppressive Immune Cell Infiltration. *Thyroid.* 2014;24(9):1385-93.

105. Lv J, Feng ZP, Chen FK, Liu C, Jia L, Liu PJ, et al. M2-like tumor-associated macrophages-secreted Wnt1 and Wnt3a promotes dedifferentiation and metastasis via activating beta-catenin pathway in thyroid cancer. *Mol Carcinogen.* 2021;60(1):25-37.

106. Lee C, Kim M, Lee JH, Oh J, Shin HH, Lee SM, et al. COL6A3-derived endotrophin links reciprocal interactions among hepatic cells in the pathology of chronic liver disease. *J Pathol.* 2019;247(1):99-109.
107. Gialeli C, Theocharis AD, Karamanos NK. Roles of matrix metalloproteinases in cancer progression and their pharmacological targeting. *Febs J.* 2011;278(1):16-27.
108. Overall CM, Lopez-Otin C. Strategies for MMP inhibition in cancer: Innovations for the post-trial era. *Nat Rev Cancer.* 2002;2(9):657-72.
109. Borst J, Ahrends T, Babala N, Melief CJM, Kastenmuller W. CD4(+) T cell help in cancer immunology and immunotherapy. *Nat Rev Immunol.* 2018;18(10):635-47.
110. Bradley LM, Dalton DK, Croft M. A direct role for IFN-gamma in regulation of Th1 cell development. *J Immunol.* 1996;157(4):1350-8.
111. Viillard JF, Pellegrin JL, Ranchin V, Schaefferbeke T, Dehais J, Longy-Boursier M, et al. Th1 (IL-2, interferon-gamma (IFN-gamma)) and Th2 (IL-10, IL-4) cytokine production by peripheral blood mononuclear cells (PBMC) from patients with systemic lupus erythematosus (SLE). *Clin Exp Immunol.* 1999;115(1):189-95.
112. Chen L, Grabowski KA, Xin JP, Coleman J, Huang Z, Espiritu B, et al. IL-4 induces differentiation and expansion of Th2 cytokine-producing eosinophils. *J Immunol.* 2004;172(4):2059-66.
113. Korn T, Bettelli E, Oukka M, Kuchroo VK. IL-17 and Th17 Cells. *Annu Rev Immunol.* 2009;27:485-517.

114. Raskov H, Orhan A, Christensen JP, Gogenur I. Cytotoxic CD8(+) T cells in cancer and cancer immunotherapy. *Br J Cancer*. 2021;124(2):359-67.
115. Barry M, Bleackley RC. Cytotoxic T lymphocytes: All roads lead to death. *Nature Reviews Immunology*. 2002;2(6):401-9.
116. Mehta AK, Gracias DT, Croft M. TNF activity and T cells. *Cytokine*. 2018;101:14-8.
117. Bhat P, Leggatt G, Waterhouse N, Frazer IH. Interferon-gamma derived from cytotoxic lymphocytes directly enhances their motility and cytotoxicity. *Cell Death & Disease*. 2017;8.
118. Kalia V, Sarkar S. Regulation of Effector and Memory CD8 T Cell Differentiation by IL-2-A Balancing Act. *Front Immunol*. 2018;9:2987.
119. Cibrian D, Sanchez-Madrid F. CD69: from activation marker to metabolic gatekeeper. *Eur J Immunol*. 2017;47(6):946-53.
120. Jewett A, Man YG, Cacalano N, Kos J, Tseng HC. Natural killer cells as effectors of selection and differentiation of stem cells: Role in resolution of inflammation. *J Immunotoxicol*. 2014;11(4):297-307.
121. Tugores A, Alonso MA, Sanchezmadrid F, Delandazuri MO. Human T-Cell Activation through the Activation-Inducer Molecule/Cd69 Enhances the Activity of Transcription Factor-Ap-1. *J Immunol*. 1992;148(7):2300-6.
122. Mita Y, Kimura MY, Hayashizaki K, Koyama-Nasu R, Ito T, Motohashi S, et al. Crucial role of CD69 in anti-tumor immunity through regulating the exhaustion of tumor-infiltrating T cells. *International Immunology*. 2018;30(12):559-67.

123. Esplugues E, Vega-Ramos J, Cartoixa D, Vazquez BN, Salaet I, Engel P, et al. Induction of tumor NK-cell immunity by anti-CD69 antibody therapy. *Blood*. 2005;105(11):4399-406.
124. Esplugues E, Sancho D, Vega-Ramos J, Martinez C, Syrbe U, Hamann A, et al. Enhanced antitumor immunity in mice deficient in CD69. *J Exp Med*. 2003;197(9):1093-106.
125. Fergusson JR, Fleming VM, Klenerman P. CD161-expressing human T cells. *Front Immunol*. 2011;2:36.
126. Rezvani K, Rouse RH. The Application of Natural Killer Cell Immunotherapy for the Treatment of Cancer. *Front Immunol*. 2015;6:578.
127. Aldemir H, Prod'homme V, Dumaurier MJ, Retiere C, Poupon G, Cazareth J, et al. Cutting edge: Lectin-like transcript 1 is a ligand for the CD161 receptor. *J Immunol*. 2005;175(12):7791-5.
128. Smyth MJ, Thia KYT, Cretney E, Kelly JM, Snook MB, Forbes CA, et al. Perforin is a major contributor to NK cell control of tumor metastasis. *J Immunol*. 1999;162(11):6658-62.
129. Wang W, Erbe AK, Hank JA, Morris ZS, Sondel PM. NK Cell-Mediated Antibody-Dependent Cellular Cytotoxicity in Cancer Immunotherapy. *Front Immunol*. 2015;6:368.
130. Hu Z, Shin HS, Kim YH, Ha SY, Kim SJ, Won JK, Park YJ, Parangi S, Cho SW, Lee KE. Modeling the tumor microenvironment of anaplastic thyroid cancer: an orthotopic tumor model in C57BL/6 mice. *Front Immunol*. doi: 10.3389/fimmu.2023.1187388.

국문초록

종양관련 대식세포에서 유래되는 endotrophin이 갑상선암

미세환경에 미치는 역할에 대한 연구

서울대학교 대학원 중개의학전공

(지도교수: 박도준)

신효식

Endotrophin (ETP)은 type VI collagen $\alpha 3$ (COL6A3)에서 C5 domain이 절단되어 생성된 단백질로써, 유방암과 간암의 종양 조직에서 정상 조직과 비교해서 높은 수치를 보이고 있으며 종양의 악성도와 관련이 있음을 보고 하고 있지만 종양 미세환경에서의 ETP의 역할에 대한 연구는 부족하다. 본 연구는 갑상선암 미세환경에서 ETP의 기원 세포를 조사하였고, ETP에 의한 갑상선 암세포의 변화와 갑상선암 미세환경에서 ETP에 의해 조절되는 유전자 및 면역세포의 분석에 대해 기술하였다. 갑상선 암세포로 자극받은 대식세포에서 ETP의 발현이 증가하였다. 또한 ETP에 의해서 갑상선 암세포

의 이동능이 증가하였다. ETP를 갑상선 암세포에 처리 후, 변화된 유전자를 확인하기 위한 RNA 시퀀싱 분석 결과에서, 세포 이동과 관련된 유전자들의 발현이 증가하였다. 또한 면역억제를 유도하는 유전자 및 혈관 신생성을 자극하는 유전자도 증가하였다. 반면에 ETP가 처리되지 않은 군에서는 면역활성을 증가시키는 유전자와 종양 억제 유전자의 발현이 증가하였다. 다음으로, 생체내 ETP의 영향을 관찰하기 위해 COL6A3가 결핍된 마우스와 정상 마우스에 각각 갑상선암을 유발하였을 때, COL6A3가 결핍된 마우스에서 갑상선암의 성장이 감소하였다. 종양을 면역화학염색으로 분석한 결과, COL6A3가 결핍된 마우스의 종양에서 세포독성 T 세포가 현저히 증가했다. 또한 종양 RNA의 분석 결과, COL6A3가 결핍된 마우스의 종양에서 면역반응을 유도하는 T 세포와 관련된 유전자의 증가와 종양 억제 역할을 하는 M1 대식세포의 유전자가 증가했다. 이러한 결과를 바탕으로, 갑상선암 미세환경의 M2 대식세포에서 유래되는 ETP가 갑상선암의 공격성을 증가시키고 면역 억제를 유도하여 종양

성장의 친화적인 환경으로 변화시킴을 증명하였다. 따라서 ETP는 대식세포가 풍부한 갑상선암의 좋은 표적 치료제가 될 수 있음을 제안한다.

주요어: endotrophin, 종양미세환경, 대식세포, 갑상선암, type VI collagen α 3

학 번: 2018-35950

감사의 글

박사 졸업을 위한 6년이라는 시간은 저에게 있어서 기적 같은 시간이었습니다. 천사 같은 저의 지도교수님이신 조선욱 교수님을 만나게 되었고 교수님으로 많은 것을 배우면서, 저의 강점을 찾을 수 있었고 부족한 점은 개선할 수 있었습니다.

그런 소중한 6년이라는 시간이 흐르는 동안 박사 학위 논문을 제출하기까지 도움을 주신 많은 분들에게 감사의 말씀을 전합니다.

우선 미흡한 저를 졸업할 수 있도록 잘 지도하고 이끌어주신 박도준 교수님께 진심으로 감사드립니다. 또한 랩미팅 시간마다 논문의 완성도를 높이고자 저의 발표에 대해서 조언을 아끼지 않으신 박영주 교수님께도 감사드립니다. 졸업 논문의 부족한 점에 대해서 좋은 말씀을 주신 심사위원 교수님이신 김재범 교수님, 이미옥 교수님, 배운수 교수님께도 깊은 감사의 말씀드립니다.

제가 실험실에 처음 왔을 때 불편하지 않도록 배려를 많이 해주시고 제가 처음 접해보는 실험을 잘 가르쳐주신 선현진 선생님께 큰 감사의 말씀을 전합니다. 논문 작성에 있어서 여러 조언들로 도움을 주신 송민경 박사님께도 감사의 인사를 드립니다. 그리고 실험에 대해서 여러 의견도 나누고 제가 성장할 수 있게 도움을 주신 갑상선 내과 연구원 선생님들께도 고맙다는 인사를 보내드립니다.

그 밖에도, 이 곳에서 박사과정을 하며 만났었던 모든 분들이 있었기에 지금의 제가 있을 수 있었습니다. 다시 한번 감사의 말씀드립니다.

마지막으로, 박사과정 동안 힘들어하는 시기에 위로와 격려로 저에게 자신감을 잃지 않도록 도와준 소중한 가족인 누나, 매형, 조카 지후와 설이에게도 고맙다는 인사를 전합니다. 또한 제멋대로인 사위를 항상 따뜻하게 보듬어주시는 장모님, 장인어른께도 감사드리고 언제나 저에게 용기를 주는 재희형에게도 감사 인사를 전해 드립니다.

누구보다 저로 인해서 고생하고 있지만, 착한 마음으로 이해해주어서 제가 좋은 결실을 맺을 수 있도록 옆에서 항상 도와주는 사랑하는 아내 주희와 40년이 넘도록 아들로서는 미흡한 저를 자랑스러워 하시고 변함없이 아낌없는 사랑을 주시는 우리 어머니, 아버지와 함께 이 결실을 나누고 싶습니다.

2023년 7월 저자 씀

Acknowledgement

본 연구는 2020년도 대한암연구재단 암연구 박사학위논문 저술 지원사업 지원에 의하여 수행 되었음.